2784-9-F

FINAL REPORT

ATTENUATION OF SOUND BY SPHERICAL SHELLS

by

Norman E. Barnett

for

COOLEY ELECTRONICS LABORATORY

Department of Electrical Engineering
The University of Michigan
Ann Arbor, Michigan

Contract No. Nonr-1224(24)
Office of Naval Research
Department of the Navy
Washington 25, D. C.

October 1966

UMR0221

ABSTRACT

The study of acoustic attenuation at low frequencies by thin spherical shells was continued beyond the initial analysis by Goodman and Stern (J. Acoust. Soc. Am., 34:338, 1962). Experimental measurements were conducted both in air and in water. Numerical evaluation was extended to include the first-order coefficient. For metallic shells immersed in either air or water, the first-order coefficient is larger than, and exhibits interesting fluctuations at lower frequencies, than, the zeroth-order coefficient. As a practical consequence, pure zeroth-order behavior is difficult to observe even in the laboratory and most measurements exhibit the combined effects from several orders.

TABLE OF CONTENTS

LIST OF ILLUSTRATIONS

1. INTRODUCTION

The physical problem under consideration involves a study of the acoustical fields which result when a plane sound wave impinges upon a complete spherical shell composed of isotropic elastic material. A particular case of the general problem, which is closely related to practical underwater acoustical engineering, occurs when the shell is immersed in and flooded with sea water. This particular case constitutes a spherical idealization of a passive sonar system in which the elastic shell plays the role of a sonar dome. A detailed study of this case offers the possibility, among others, of critically examining the role of the shell's material parameters as they affect the acoustic intensity transmitted into the interior space. It will become evident that the role of the shell is much more complex than is predicted using the more conventional considerations of sound transmission through layered media. In addition to sonar problems, there are many other practical situations which can be approximated and then studied in detail by utilizing an appropriate spherical-shell model.

From the standpoint of pure physics, the spherical-shell problem goes far beyond the fundamental considerations of the transmission of sound through a three-layered medium. By virtue of its geometry, the spherical-shell problem involves an enclosed space of finite dimensions and eigen values appropriate to that geometry appear in the solution. Furthermore, the shell material is considered to be a physical solid possessing finite shear stiffness and, as a consequence, the characteristic impedance of the shell material is not a sufficient parameter to characterize its acoustical behavior. Through these essentials, a spherical shell configuration constitutes the simplest complete physical representation of an acoustical enclosure and, therefore, it is an appropriate model for the study of the elementary physics of acoustical enclosures.

Much of the importance attached to the spherical-shell model derives from the fact that it is amendable to a detailed theoretical analysis and because the mathematical solutions are in closed form. (Shells possessing nonspherical geometrics generally are

less tractable mathematically although the physics of the situation must remain essentially similar to that for the spherical shell.) Several investigations have considered portions of the spherical-shell problem or closely related problems. For example, Rayleigh discussed the scattering of plane sound waves by a spherical obstacle (Ref. 1). Anderson has treated the scattering of sound from a fluid sphere (Ref. 2). More recently, Goodman and Stern have analyzed the spherical-shell problem from the standpoint of classical potential theory and, in particular, have given an explicit expression for the acoustical field internal to the shell (Ref. 3; also Refs. 4, 5). The research described in this report rests most directly on their work. Hickling has also published recently concerning the scattered field from a solid spherical obstacle (Ref. 6) and from an elastic spherical shell (Ref. 7). Likewise, some recent experimental research has been reported (Refs. 8, 9) which relates directly to the theoretical treatments of the scattered field in Refs. 6 and 7, respectively.

So far as is known, only the work of Goodman and Stern has explicitly treated the acoustical field interior to the spherical shell (Ref. 3). Hickling's paper (Ref. 7) implicitly includes the interior field also, since his analysis is similar to that used in Ref. 3. However, he directed his attention exclusively to the scattered field and derived only those solutions relating explicitly to the exterior field. His equations would have to be solved again for a different set of coefficients to extract information about the interior field.

Goodman and Stern (Ref. 3) devote the major portion of their discussion to the external scattered field and demonstrate that appropriate limiting cases correlate with more specialized analyses by other investigators. Of most importance to the present report, however, is the fact that Goodman and Stern provide an exact analytical expression for the acoustic pressure; or alternatively, for the acoustic intensity, within an elastic spherical shell when it is immersed in and filled with the same ideal fluid. Liquid sea water was the archetype fluid but in their general analysis, no special restrictions were imposed on the ideal fluid beyond assuming that the same fluid existed on both sides of the shell. (Even the assumption of identical ideal fluids could be dropped at the expense of some algebraic complexity).

After deriving an exact expression for the interior acoustical field, Goodman and Stern specialize their analytical results to the low-frequency approximation which holds at the center of a thin spherical shell. As would be expected, various higher-order

mathematical terms were discarded in the course of developing these approximations. Most of the discarded terms belonged to the series expansions for the spherical Bessel and Neumann functions but some of the decisions to discard terms may have been based on magnitude comparisons involving the material parameters which characterize the fluid and the shell. Consequently, one must adhere strictly to the general intent of the approximate solutions, i. e., thin shell of solid material in water, low frequencies, and center of shell. The alternatives are either to employ the general form of the solution with its complicated coefficients or to reevaluate the approximations, making explicit the physical consequences of each mathematical step. For example, it is not immediately certain if the approximate value of the coefficient A_0^{III} given by Goodman and Stern (Ref. 3, Eq. 22a) may be applied to a metal shell in air although their general formulation certainly admits this case.

2. BASIS FOR PRESENT RESEARCH

As has been noted, the present research rests directly upon the analytical expression obtained by Goodman and Stern for the acoustical field interior to a spherical shell. The geometry of the problem is defined in Fig. 1 and the scalar potential applying to the fluid contained within the shell was expressed as: (Ref. 3, Eq. 4c):

$$\phi_{III} = \sum_{\ell=0}^{\infty} A_\ell^{III} P_\ell(\cos\theta) j_\ell(kr) \qquad (1)$$

where:

ϕ_{III} = scalar potential function for the fluid inside the spherical shell

A_ℓ^{III} = coefficients for the interior field

$P_\ell(\cos\theta)$ = Legendre polynomials (expressing all directional variations)

$j_\ell(kr)$ = spherical Bessel function (expressing all radial variation)

r, θ = coordinates of a point in the interior space $0 \leq r \leq R - \Delta$ and $0 \leq \theta \leq III$

k = ω / c = wave number

ℓ = mathematical order of the functions

R = outer radius of the spherical shell

Δ = thickness of the spherical shell

III = designation of the interior space when used either as subscript or superscript (in contrast to the exterior space, designated by I and the shell, designated by II.)

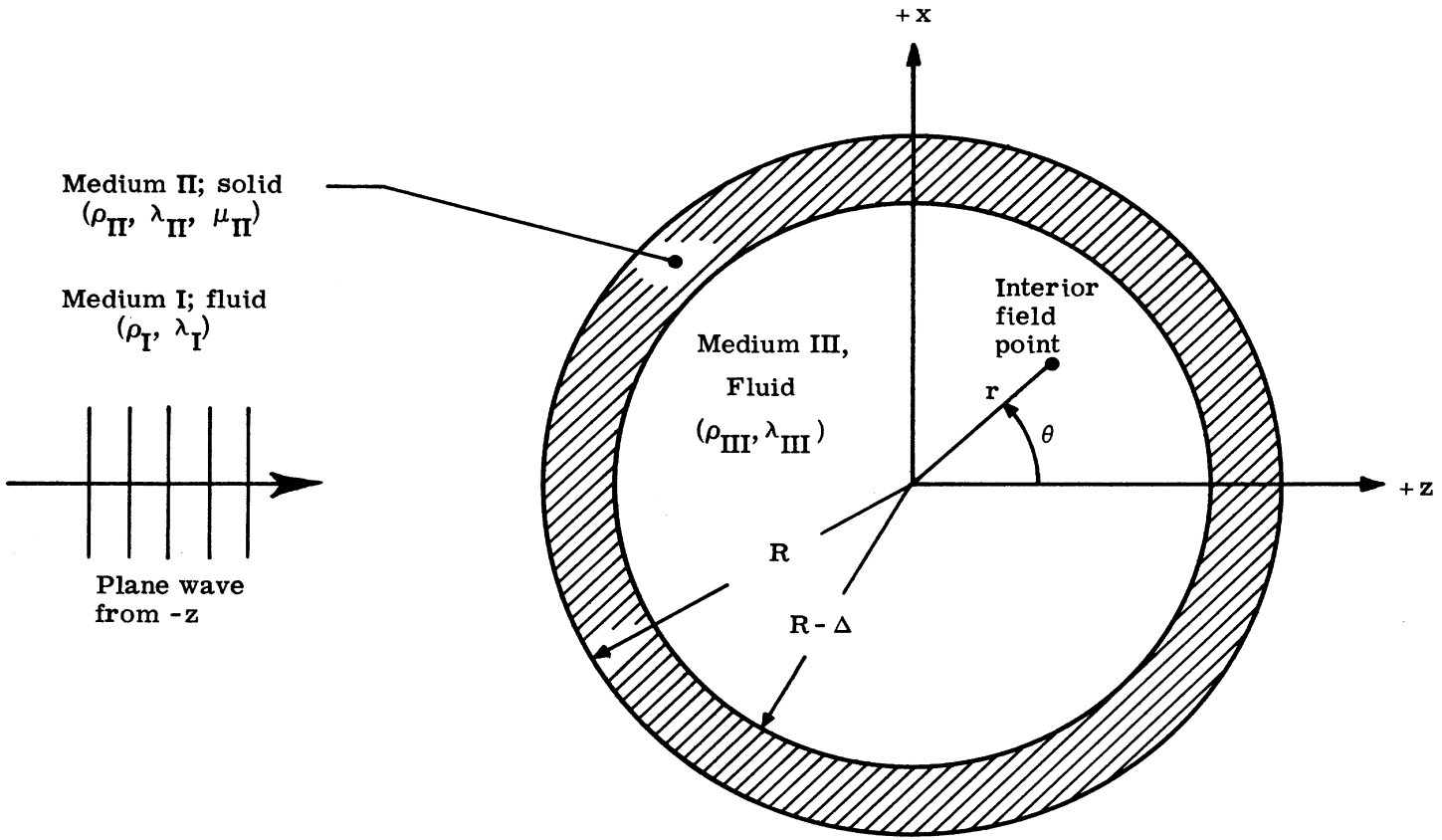

Fig. 1. Spherical shell model for analysis.

The coefficient A_ℓ^{III} is (Ref. 3, Eqs. 21A and 21b):

$$A_\ell^{III} = i^\ell (2\ell+1) \frac{\begin{vmatrix} \alpha_{11} & \alpha_{12} & \alpha_{13} & \alpha_{14} & \alpha_{15} & a_1 \\ \alpha_{21} & \alpha_{22} & \alpha_{23} & \alpha_{24} & \alpha_{25} & a_2 \\ 0 & \alpha_{32} & \alpha_{33} & \alpha_{34} & \alpha_{35} & 0 \\ 0 & \alpha_{42} & \alpha_{43} & \alpha_{44} & \alpha_{45} & 0 \\ 0 & \alpha_{52} & \alpha_{53} & \alpha_{54} & \alpha_{55} & 0 \\ 0 & \alpha_{62} & \alpha_{63} & \alpha_{64} & \alpha_{65} & 0 \end{vmatrix}}{\begin{vmatrix} \alpha_{11} & \alpha_{12} & \alpha_{13} & \alpha_{14} & \alpha_{15} & 0 \\ \alpha_{21} & \alpha_{22} & \alpha_{23} & \alpha_{24} & \alpha_{25} & 0 \\ 0 & \alpha_{32} & \alpha_{33} & \alpha_{34} & \alpha_{35} & 0 \\ 0 & \alpha_{42} & \alpha_{43} & \alpha_{44} & \alpha_{45} & \alpha_{46} \\ 0 & \alpha_{52} & \alpha_{53} & \alpha_{54} & \alpha_{55} & \alpha_{56} \\ 0 & \alpha_{62} & \alpha_{63} & \alpha_{64} & \alpha_{65} & 0 \end{vmatrix}} \qquad (2a)$$

for $\ell \geq 1$

and

$$A_o^{III} = \frac{\begin{vmatrix} \alpha_{11} & \alpha_{12} & \alpha_{14} & a_1 \\ \alpha_{21} & \alpha_{22} & \alpha_{24} & a_2 \\ 0 & \alpha_{42} & \alpha_{44} & 0 \\ 0 & \alpha_{52} & \alpha_{54} & 0 \end{vmatrix}}{\begin{vmatrix} \alpha_{11} & \alpha_{12} & \alpha_{14} & 0 \\ \alpha_{21} & \alpha_{22} & \alpha_{24} & 0 \\ 0 & \alpha_{42} & \alpha_{44} & \alpha_{46} \\ 0 & \alpha_{52} & \alpha_{54} & \alpha_{56} \end{vmatrix}} \qquad (2b)$$

where a_1, a_2, and α_{ij} are functions of the material parameters and dimensions as given in detail in Appendix A. Although the above expressions are exact for the assumed physical model, it is evident that they are so complicated that it will be very difficult to evaluate the roles of individual parameters. For small shells of arbitrary thickness, an approximate evaluation of the coefficients A_ℓ^{III} leads to (Ref. 3, Eqs. 22a and 22b):

$$A_0^{III} \cong \frac{-3\lambda_I(\lambda_{II} + 2\mu_{II})}{4\mu_{II}(\lambda_{II} + \frac{2}{3}\mu_{II} - \lambda_I)(1 - \xi^3) + 3\lambda_I(\lambda_{II} + 2\mu_{II})} \tag{3a}$$

$$A_1^{III} \cong \frac{9i(\frac{\rho I}{\rho II})}{\frac{3\rho I}{\rho II} + 2(1 - \frac{\rho I}{\rho II})(1 - \xi^3)} \tag{3b}$$

where

$$\xi = 1 - (\frac{\Delta}{R})$$

The sound intensity in the interior space is

$$I = |\phi_{III}|^2 \tag{4}$$

and, as Goodman and Stern point out (Ref. 3, Eq. 23), if attention is restricted to the field at or very near to the center of the spherical shell:

$$I \cong |A_0^{III}|^2 \tag{5}$$

It was at this juncture that it was decided to attempt an experimental verification of the accuracy and adequacy of these analytical results. Eq. 5 above asserts that to a first approximation at low frequencies and at the center of the shell, the sound intensity is governed by the square of the magnitude given by Eq. 3a or, alternatively, that Eq. 3a directly represents the sound pressure. At first glance, this assertion appears quite foreign to the usual transmission loss situation because Eq. 3a is comprised exclusively of Lamé constants and shell dimensions; density does not appear.

In the case of sound transmission at normal incidence through, a steel plate, for example, immersed in water, ordinarily on the basis of layered media considerations

one obtains an expression of the form (see Ref. 10, p. 138, Eq. 6. 37a):

$$\alpha_t \cong \frac{4}{4\cos^2(k_2 \ell) + \left(\frac{\rho_2 c_2}{\rho_1 c_1}\right)^2 \sin^2(k_2 \ell)} \tag{6}$$

where

α_t = intensity transmission coefficient = $\frac{\text{intensity transmitted}}{\text{intensity incident}}$

$\rho_1 c_1$ = characteristic impedance of the fluid (density, velocity of sound respectively)

$\rho_2 c_2$ = characteristic impedance of plate of solid material

ℓ = thickness of the plate

k_2 = wave number in the plate = $\frac{\omega}{c_2}$

or, for a thin plate at low frequencies, $k_2 \ell << 1$,

$$\alpha_t \cong \frac{(2\rho_1 c_1)^2}{(2\rho_1 c_1)^2 + (\rho_2 \omega \ell)^2} \tag{7}$$

which expression leads to the mass law of architectural acoustics when the fluid medium is air. In these cases, the transmitted intensity is governed by parameters including density, velocity, frequency, and thickness. By identifying:

$$c_1 = \sqrt{\frac{\lambda_1}{\rho_1}}$$

the above equation can be rewritten as:

$$\alpha_t \cong \frac{4\rho_1 \lambda_1}{4\rho_1 \lambda_1 + (\rho_2 \omega \ell)^2} \tag{7a}$$

so that the Lamé constant λ_1 appears explicitly in place of the propagation velocity, c_1. Sound transmission through plates as described by Eqs. 6 and 7 has been thoroughly studied and need not be discussed further here; the adequacy and limitations are well-known.

In contrast to the above, the form of Eq. 3a is quite foreign and therefore needs

explanation and verification. (Goodman and Stern have assumed that the incident plane wave has unity amplitude and consequently $|A_0^{III}|^2$ effectively represents the transmission ratio for the spherical-shell.) Analytically, the different results are not surprising. The initial models are very different and moreover, the spherical-shell model includes shear stiffness through assigning a finite value to μ_{II}: For the spherical-shell model at low enough frequencies, the behavior should be stiffness controlled and ought to differ from a mass-controlled description.

Nevertheless, it feels slightly strange for mass or density to be so conspicuously absent. True, density reappears in Eq. 3b, but the mathematical contribution of this term and of all higher order terms vanish at the center of the shell. Experimentally, the statement of Eq. 3a is even less familiar and therefore demands explanation and verification. Moreover, there are practical implications. Sonar dome materials ordinarily are selected and engineering designs executed on the basis of matching the characteristic impedance of water; a reasoning based on Eq. 6. However applicable the precepts of Eq. 6 may be for plane windows of solid materials at higher frequencies, Eq. 3a implies otherwise for curved windows at low frequencies.

Goodman and Stern continued their studies by considering a hemispherical shell mounted on a rigid plane of infinite extent. In that case, the intensity near the center of a hemispherical shell became (Ref. 3, Eq. 28):

$$I_{\text{hemisphere}} \cong \left|2A_0^{III}\right|^2 \tag{8}$$

(Eq. 8 represents simply the analytical expression for pressure-doubling at a rigid boundary.) They concluded their presentation with several graphs for particular cases of hemispherical shells (selected radii, thickness, and shell material) immersed in sea water. They plotted $10 \log_{10}\left|2A_0^{III}\right|^2$ along the ordinate against frequency as abscissa. Because unity was selected as a reference magnitude, the complete absence of a shell (or for a shell "constructed" of sea water) led to an intensity level of +6.02 db on their graphs. Thus the predicted attenuation (or gain) is displayed on those graphs by the amount the curves depart from a level of +6.02 db. Miss Stern has published a larger collection of such graphs in Ref. 5.

Figure 2 reproduces the calculated results for a complete spherical shell made from steel 3/8-inch thick and two feet in outer radius. The ordinate values used in Fig. 2 are $-20 \log_{10} \left| \frac{A_0^{III}}{1} \right|$ and thus represent the acoustical intensity to zeroth order at the center of a complete spherical shell as given by Eq. 5. In the absence of a shell, the intensity level would be zero decibels. Thus positive values of the ordinate in the graph represent attenuation due to the shell. The long-dash line was obtained by using Eq. 3a while the solid line was obtained by using Eq. 2b to evaluate A_0^{III}. (Figure 2 is essentially the same as Fig. 11 in Ref. 5 displaced downward by 6.02 db.) The short-dash line indicates the attenuation which would be predicted for 3/8-inch steel plate using Eq. 6.

The original point of departure for this experimental research was to explore the agreement with the analytical results depicted in Fig. 2. At low frequencies, all of the particular cases presented in Ref. 5, yielded results similar to those in Fig. 2; namely:

(a) at very low frequencies, the curve was horizontal,

(b) at very low frequencies, the level of the curve represented attenuation of small magnitude,

(c) with increasing frequency, the curve first dipped to a shallow minimum (at about 550 cps in Fig. 2) and then climbed rather steeply,

(d) at still higher frequencies, more complicated behavior appeared but reservations were expressed in Ref. 5 about whether the computed values were accurate in this region and whether the zeroth-order term was still preponderate.

The magnitude of attenuation at very low frequencies increased with increasing shell thickness and decreased with increasing shell radius. The magnitude of this attenuation also varied with type of shell material. For the real materials which were studied in Ref. 5, the parameters λ, μ, and ρ all varied simultaneously so that it was difficult to comprehend their individual effects in isolation. For example, Lucite contributed the smallest attenuation presumably because its values of λ and ρ were most like sea water but simultaneously, its value of μ was also the smallest among the several materials. In this instance, the results are consistent with conclusions drawn on the elementary basis of matching acoustical impedance. They do not clearly reveal what, if anything, the introduction of

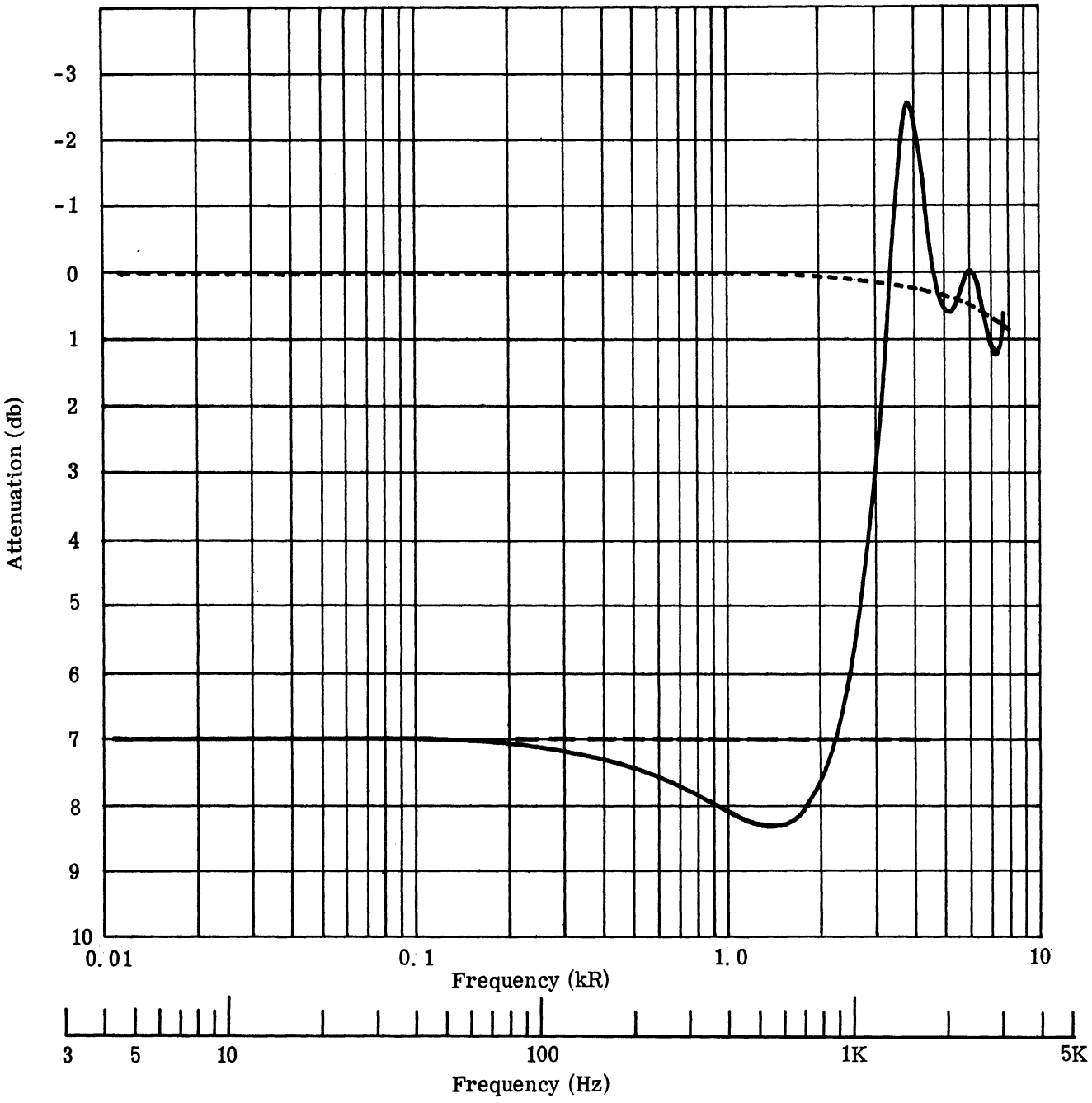

Fig. 2. Zeroth-order analytical prediction for steel shell immersed in water.

solid characteristics, namely, a finite value of μ, has contributed to the understanding of the problem.

It was decided to undertake some experiments to see if the general features displayed in Fig. 2 could be verified. Thus, the initial idea was to observe the sound pressure at the center of a thin spherical shell as a function of frequency and to see if we could obtain the predicted curve; that is, a small and constant amount of attenuation at lowest frequencies and then a dip followed by an abrupt increase at higher frequencies. Because the predicted low-frequency attenuation for a shell in sea water amounted to a few decibels at most, consideration had to be given to obtaining extraordinarily precise relative measurements, reliable to perhaps one-tenth of a decibel. Less precise measurements would not suffice for validating the analytical predictions.

The radius of a shell enters the analysis only through the arguments of the spherical Bessel and Neumann functions, more specifically, it appeared only in the nondimensional expression, $\frac{\omega R}{c}$. Apparently any convenient value of radius may be selected for the experimental studies provided only that the frequency range is adjusted accordingly, or conversely, the radius may be chosen to fit a particular frequency range. The auxiliary frequency scale in Fig. 2 emphasizes this consideration and is intended to suggest that much of our experimental work was accomplished with 3-inch radius shells. Initially, it was felt that two shells identical except for thickness (say, 4-inch radius stainless steel, 0.037-inch and 0.078-inch thick) and another shell of different material (say, 3-inch radius copper, 0.022-inch thick) would suffice for experimental comparison with the analysis.

A variety of pressed or spun metal shells were acquired from several sources (commercial products for which tooling existed) and exploratory experiments undertaken.[1] A small anechoic water tank was designed and constructed to assist the research (see Ref. 11). This anechoic tank was intended to provide characteristics suitable for preliminary studies whereas the final definitive data were to be taken later at one of the Navy's free-field transducer calibration facilities such as the one at Pond Oreille Lake, Idaho.

---

[1]The spherical or rather hemispherical shape is difficult to draw, press, or spin free from ripples. Both prolate and oblate spheroidal shapes are easier to fabricate.

The envisioned final data have not been collected because the problem turned out to be more complex than anticipated. Nevertheless, the laboratory research has provided considerable information about the behavior of acoustical fields inside spherical-shells. Moreover, the various difficultiesencountered forced a more detailed interpretation of the analytical results which originally were considered to be complete. By hindsight, it is now clear that for most physically realizable experimental situations (sonar applications included), the zeroth-order term is not sufficient even at low frequencies. What originally appeared to be a straight-forward experimental study gradually evolved into a more detailed study and interpretation of the original analysis.

3. EXPERIMENTAL STUDIES

The several following subsections report specific aspects of the studies on spherical shells. Actually, these several categories of research were pursued more or less simultaneously but are organized according to physical considerations rather than according to chronological history.

3.1 Shells In Air And Filled With Air. The sponsored research reported in Refs. 4 and 5 was oriented toward shells immersed in sea water, i. e., a generalized sonar problem. However, when starting the experimental studies, it was recognized that the analytical solution in its most general form must encompass shells immersed in air. Consequently appropriate experiments in air could also be used to test the analytical results. Indeed, some types of measurements appeared easier to accomplish in air than in water and gave promise of displaying certain aspects of the problem more clearly than experiments in water.

The initial undertaking for studies of shells in air had to be a calculation based on Eqs. 2b, 3a, and 5 corresponding closely to experimental conditions. Thin copper shells, fabricated by two different methods, were available and so calculations were performed for their parameters and dimensions which are listed in Table I. The actual shells consisted of two hemispherical segments which slightly overlapped at the equator. They were joined either with glue (radio service cement) or soft solder. The low-frequency results computed from the parameter values in Table I are shown in Figs. 3 and 4 which have essentially the same format as used previously in Fig. 2. Equation 3a is seen to yield the correct asymptotic values for these two shells in air.[2]

The curves displayed in Figs. 3 and 4 resemble those applying to metal shells in water except that in air the magnitude of the attenuation is very much larger. In fact, the attenuation for these shells is inconveniently large from the standpoint of routine airborne sound measurements.

---

[2] These results were obtained by Miss Stern. The calculations were performed on an IBM 709 system programmed to produce A_0^{III} as defined in Eq. 2b.

TABLE I

COPPER SHELLS IN AIR

Material	Density ρ, kg/m^3	Lame constants λ, N/m^2	μ, N/m^2
Air	1.29	$1.54\times10^{+5}$	0
Copper	8890	$1.31\times10^{+11}$	$4.60\times10^{+10}$
Shell	**Fabrication**	**Radius R, m**	**Thickness Δ, m**
A	spinning	7.62×10^{-2} (3")	5.59×10^{-4} (0.022")
B	drawing	7.62×10^{-2} (3")	3.56×10^{-4} (0.014")

A variety of experiments were performed with the copper shells in air. Some measurements were conducted outdoors under approximately free-field conditions and with an incident plane wave. Other measurements were performed in the diffuse field of a reverberation room. Likewise several microphone types, crystal, dynamic and condenser, were employed to measure the internal sound pressure level resulting from a given external sound signal. All of these measurements indicated a large attenuation at low frequencies of the order of 40 to 70 db but never quite as large as predicted in Figs. 3 and 4. Moreover, all experiments gave a different frequency dependence than predicted; namely, a gradual but continuing rise with frequency, terminating in a pronounced peak at about 1500 cps. Figure 5 displays the results from one of the better early measurements performed in the reverberation room on copper shell B.[3] The signal-to-noise ratio was at least 10 db under the worst conditions and, in this measurement, the internal microphone was an Altec Type 21-C operated on a compact cathode follower built especially for this study. The dashed curve indicates the purely theoretical A_0^{III} prediction.

[3] An attempt has been made to reproduce the jaggedness of the line drawn on the x-y recorder. This jaggedness is a normal consequence of the use of a reverberation room and selected time-constants of the instrumentation. In later curves, this fine structure is disregarded by drawing an average curve.

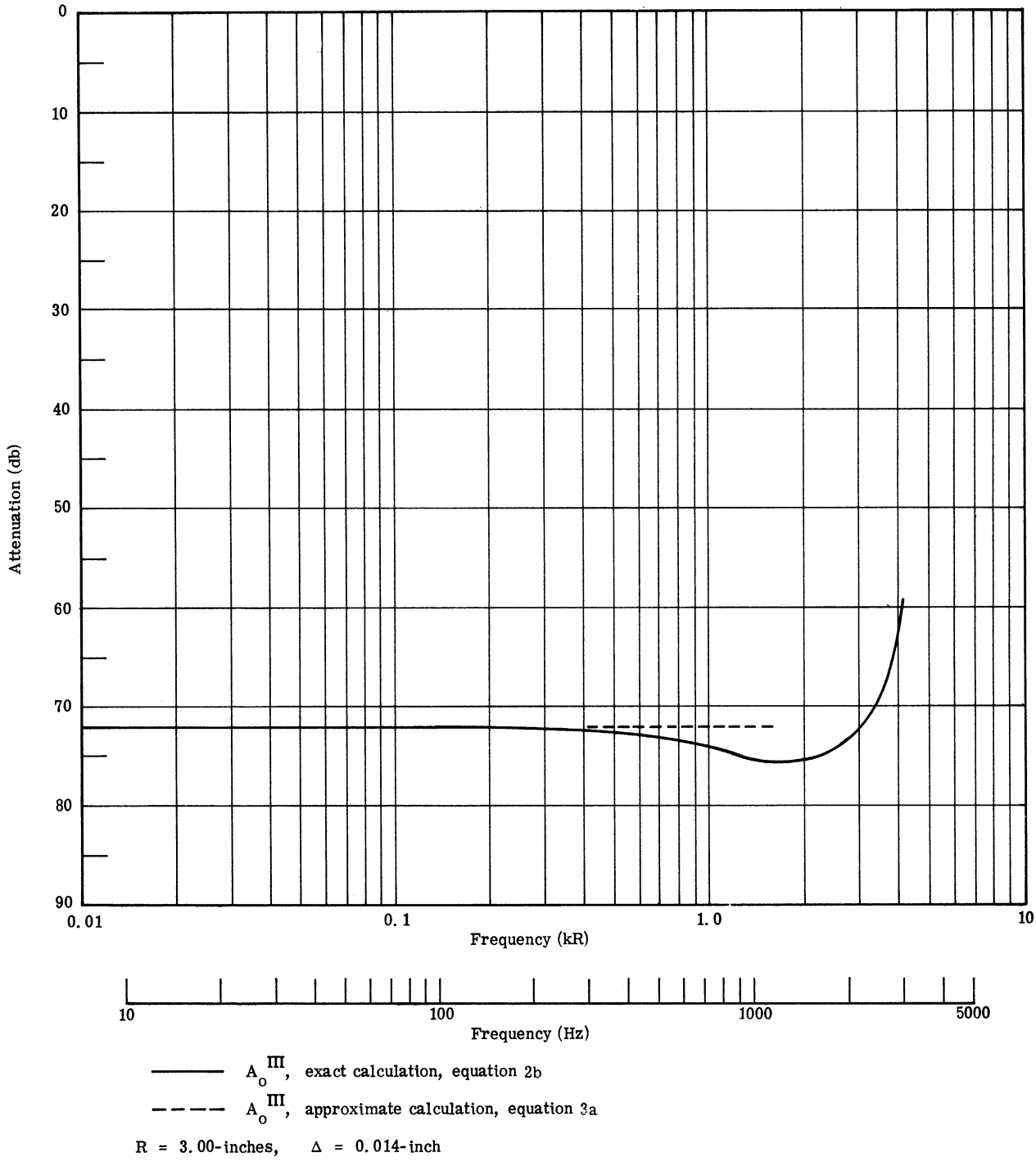

Fig. 3. Zeroth-order analytical prediction for copper shell B in air.

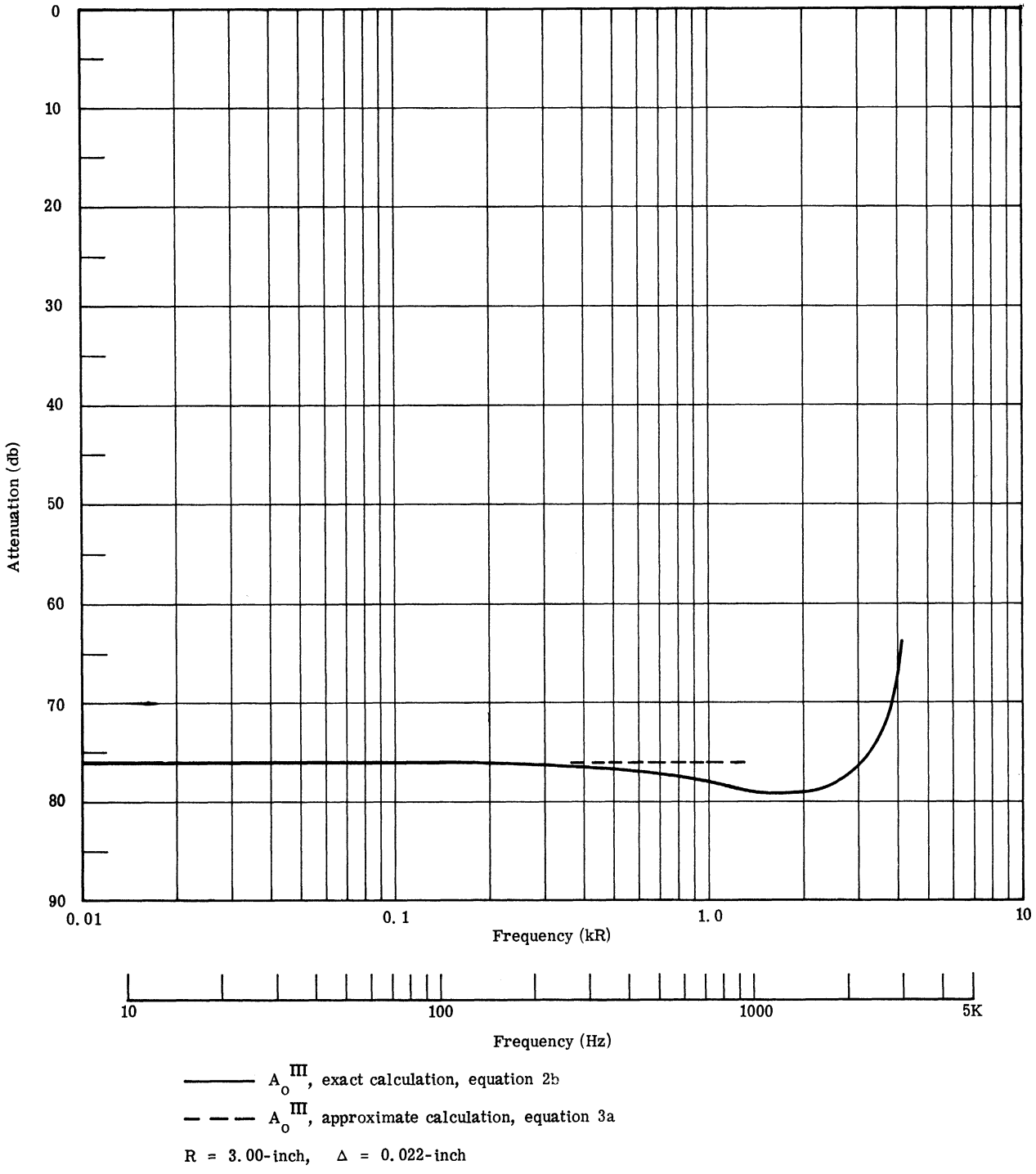

Fig. 4. Zeroth-order analytical prediction for copper shell A in air.

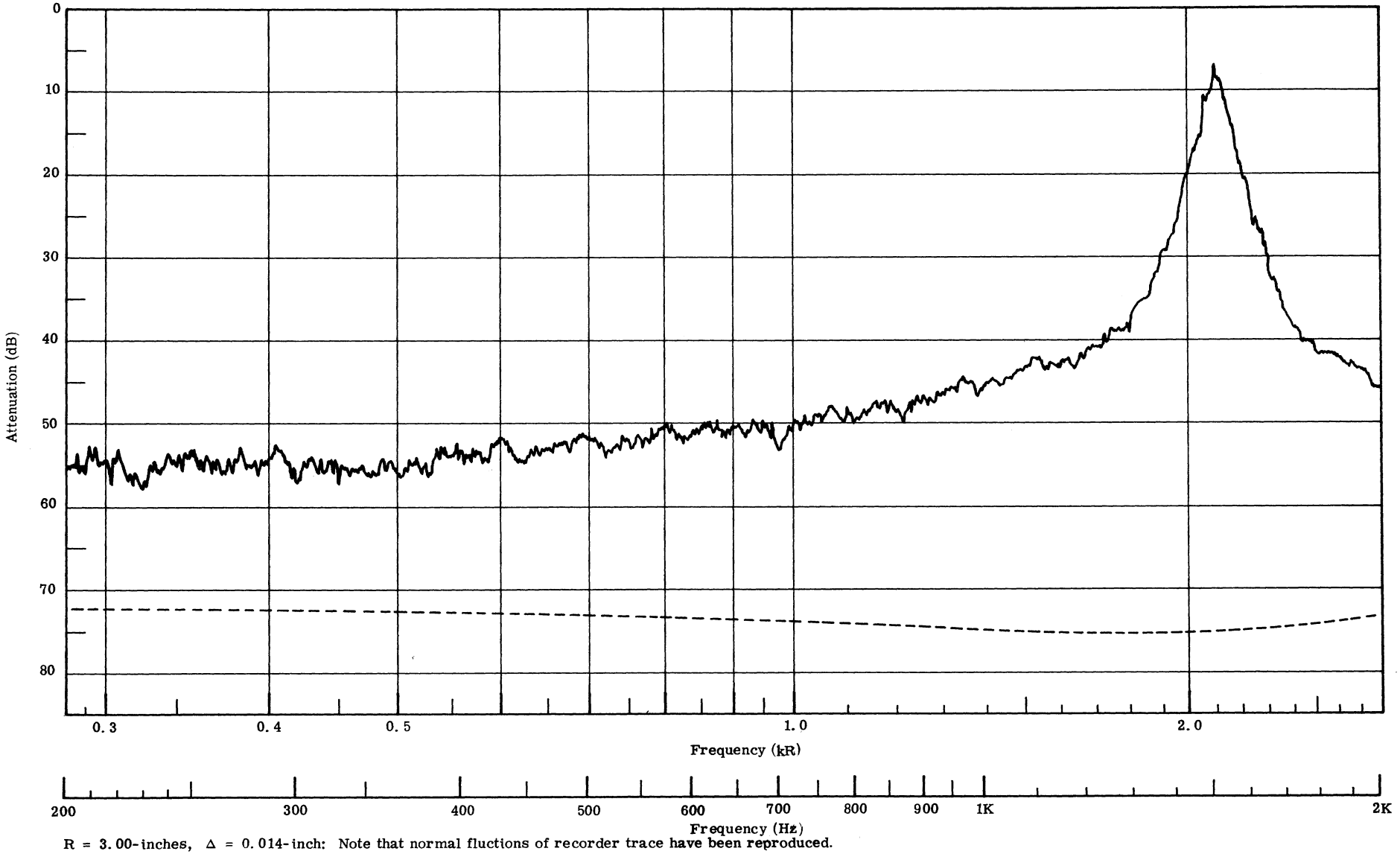

R = 3.00-inches, Δ = 0.014-inch: Note that normal fluctions of recorder trace have been reproduced.

- - - - A_o^{III} exact calculation prediction

Fig. 5. Early experimental results for copper shell B in diffuse airborne sound field.

Commercial cathode followers were too gross to place inside the spherical shell and still be able to position the microphone's diaphragm at the center of the shell. Electrically, the more compact cathode follower was similar to the General Radio Type 1551-P1-25 Microphone Base and it was operated from a General Radio Type 1551-P1-30 Power Supply. Ordinary cathode follower constructions did not have as large an acoustical attenuation as the spherical shell so they could not be allowed to project outside the shell. Also, it was not desirable to cut a hole through the shell large enough to pass the commercial units or even the large cable attached to them. Several types of microphones were used, motivated partly by uncertainty about the effect of each microphone's finite acoustical impedance upon measurements in a closed cavity. Likewise, the outdoor "plane-wave" experiments were tried to see if they would uncover some fault in a line of reasoning which concluded that the results from diffuse-field measurements in the reverberation room would be directly comparable to the analytical plane-wave solution; a point discussed in more detail below. There were a variety of other reservations related to how closely experimental conditions conformed to the ideal mathematical model, e. g., closeness to center of shell, physical intrusion into the interior space by the volume of the microphone, effect of the seam on the equator of the shell, effect of the hole cut in the shell to pass the microphone cable, effect of slight departures from a strictly spherical shape, etc.

Nevertheless, Fig. 5 represented the most reliable experimental result and it certainly contradicted much that was expected on the basis of the zeroth-order coefficient as given in Fig. 4. The peak at 1500 cps was identified as occurring at the frequency of the lowest normal mode for a spherical cavity as given by Rayleigh (Ref. 1, p. 265). At this stage, the anechoic water tank was ready for use and so work in air was discontinued in favor of measurements in water. Ultimately, further studies in air became an essential aid in clarifying a variety of outstanding problems.

The use of a reverberation room for conducting airborne sound measurements on spherical shells was mentioned above and the justification for such diffuse-field measurements may be argued as follows. The mathematical model, diagrammed in Fig. 1, required that a plane sound wave be incident from the negative z-direction. Much of the detail, however, represents merely analytical convenience and need not necessarily be carried over into the experimental activity. First, the shell is completely symmetric about its

center and so the direction chosen for the z-axis is immaterial. Furthermore by invoking superposition, plane waves arriving from any number of directions could be accommodated. In the extreme, waves could arrive from all directions with any phase relationship creating a diffuse field at the location of the shell and still the interior field would be predictable on the basis of superposition of the solutions already available. The higher orders of the solution have particular directionalities associated with them through the P_ℓ (cos θ) terms. In the case of diffuse fields, these would integrate out to particular constant average values leaving only the radial variation prescribed by the j_ℓ (kr) terms for $r \leq R - \Delta$. Moreover, in the present problem, we presumably are interested primarily in the zeroth-order term which has no directionality since $P_0(\cos \theta) \equiv 1$. Consequently, to zeroth order, experimental measurements performed in a diffuse field ought to yield precisely the same answer as the analytical solution for a plane wave incident from a specific direction. In the case of higher-order terms, a particular constant occurs for each order which is the result of integrating the P_ℓ with respect to θ.

Our laboratory is equipped with a 5400 cubic foot reverberation room and employs a rotating vane to accomplish "pure-tone" diffusion. Based on the above reasoning and confirmed by experimental evidence, this reverberation room facility can be used effectively for precise measurements on spherical shells in air which can be compared directly with the analytical predictions. Obviously, a good anechoic chamber could be utilized also but such a facility was not as conveniently available.

The most crucial question, when again undertaking measurements in air, was what pressures were acting upon the interior microphone. The observation that the peak at 1500 cps corresponded in frequency to the lowest normal mode for a spherical cavity suggested that the interior space of a metallic shell in air might behave almost like a rigid spherical cavity. That is, the impedance of the shell would be so large compared to air that a rigid cavity approximation would be valid. (Not necessarily true in water.) Thus in air, one might expect that the frequencies of the normal modes and the ordering of the normal modes would correlate with those for a rigid spherical cavity. The amplitudes of the modes could not be predicted in this way since, in reality, they would be governed by A_ℓ^{III}.

At this point, closer attention was directed to the form of the analytical result

(see Eq. 1), concentrating particularly on the function j_ℓ (kr). For convenient reference, several of the lowest-orders are graphed in Fig. 6 (see Ref. 12). In the case of a spherical cavity with rigid walls, the particle velocity must vanish at the walls; thus eigen values occur whenever zero slopes occur in Fig. 6.

First, j_0 has a zero slope at a zero-value of the argument. Because the internal radius of the cavity is finite, the argument can only vanish at zero frequency so this result appears to constitute the analytical realization of Pascal's law for this spherical model. With increasing values of the argument, the next zero slope occurs in the first-order term at $kr \cong 2.1$ This corresponds to the lowest-frequency mode for a rigid

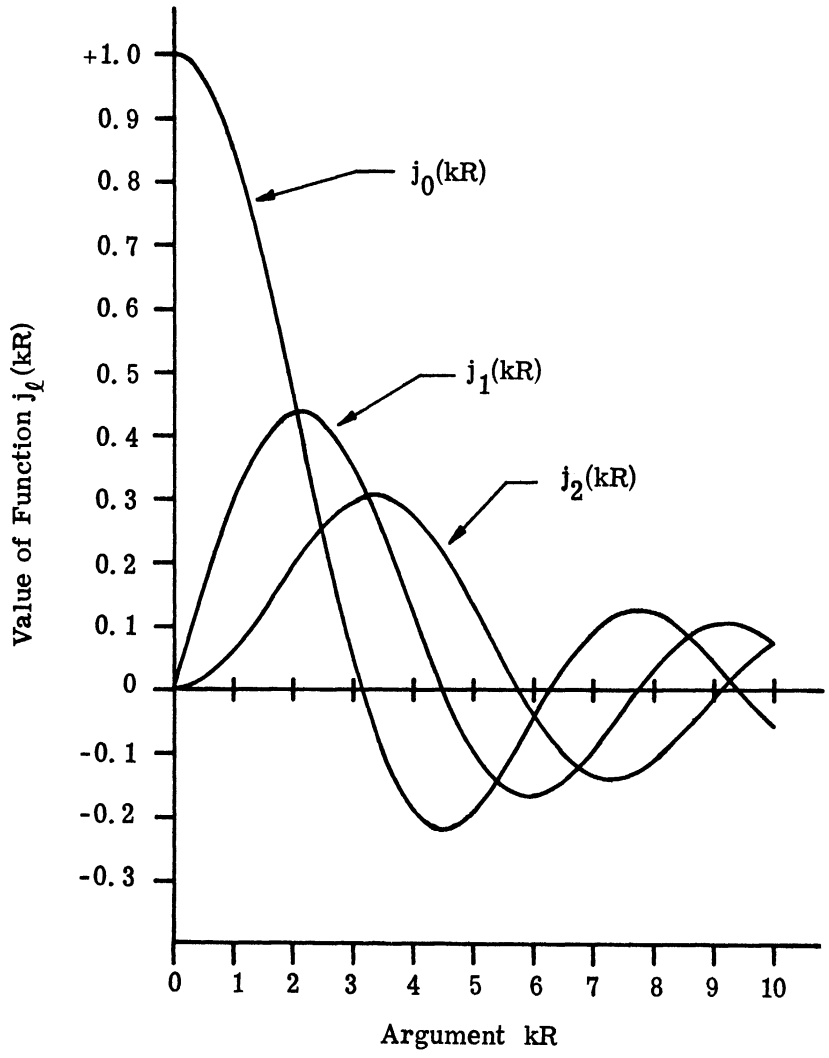

Fig. 6. Spherical Bessel functions; low order and small argument.

spherical cavity described by Rayleigh and correlates with the peak in Fig. 5. Continuing to increase the argument, the next zero slope occurs in the second-order term and then there follows a zero slope in the zeroth-order term. The important point is that when making experimental measurements by sweeping upward in frequency, the first normal mode which may be observed for an almost rigid boundary corresponds to order $\ell = 1$ and not $\ell = 0$.

Further experimentation with the copper shells produced the results displayed in Figs. 7 and 8. These measurements were obtained in a diffuse external field generated in the reverberation room. The internal microphone (an Altec 21B mounted on a miniaturized cathode follower mentioned previously) was suspended on soft rubber bands and positioned to locate the microphone's diaphragm at the center of the spherical cavity. Errors in centering the diaphragm were estimated to be less than $\pm\frac{1}{50}$ shell radius ($\pm\frac{1}{16}$").

As Figs. 7 and 8 illustrate, various normal modes were observed at the frequencies expected for a rigid spherical cavity of the same dimension. The three lowest-frequency modes were resolved cleanly. At higher frequencies, some modes occur close together and this clustering accounts for the ragged tops on several of the experimental maxima. Clearly, in this experimental situation, modes due to first- and second-order terms have not been avoided by attempting to measure the sound pressure at the center of the spherical shells. Indeed, from an examination of these results, one would judge that all of the lower modes are excited about equally strongly.

The attenuation curve for the thicker shell A consistently lies below the curve for the thinner shell B by 4 or 5 decibels when equivalent test conditions are obtained. (Figures 7 and 8 do not display this results clearly because the low-frequency portion of Fig. 8 is sloping rather than horizontal.) This direction of change would be expected from reasoning based upon either increased massiveness or increased stiffness. The magnitude of the change suggests mass as the controlling parameter but this evidence is much too weak to consider as definitive.

After locating the mode frequencies, it became experimentally possible to verify the mode identification of the three lowest-frequency modes by investigating the radial distribution of sound pressure. A probe-tube microphone system possessed sufficient attenuation through its housing to permit interpretable measurements at a mode frequency

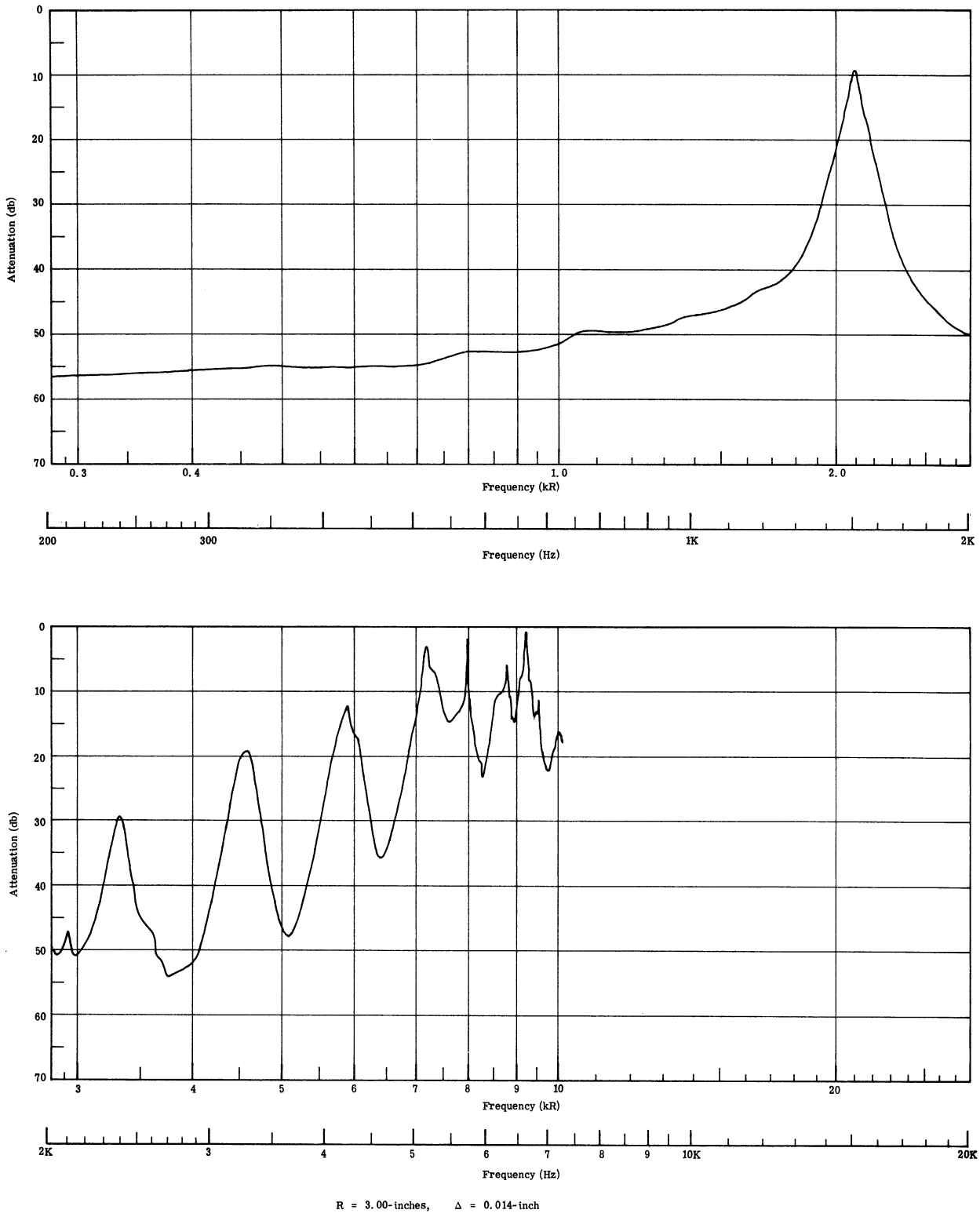

Fig. 7. Experimental results for copper shell B in air.

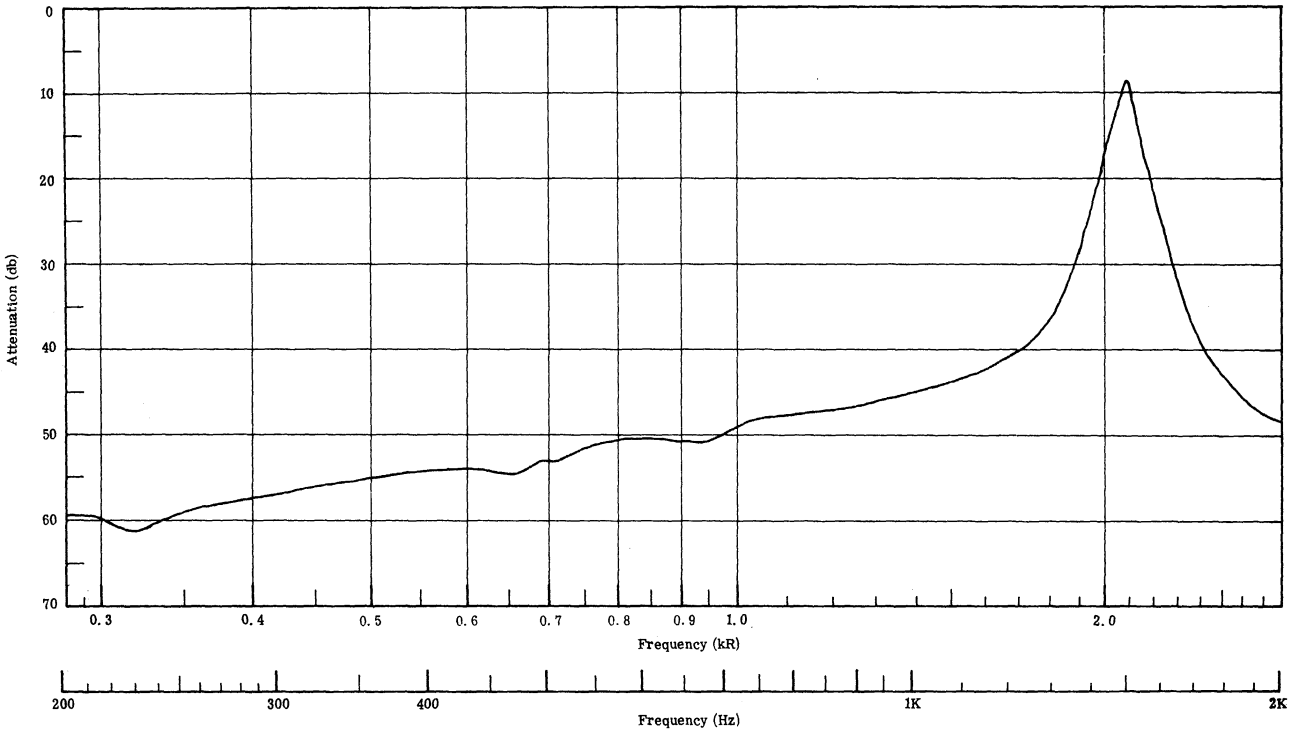

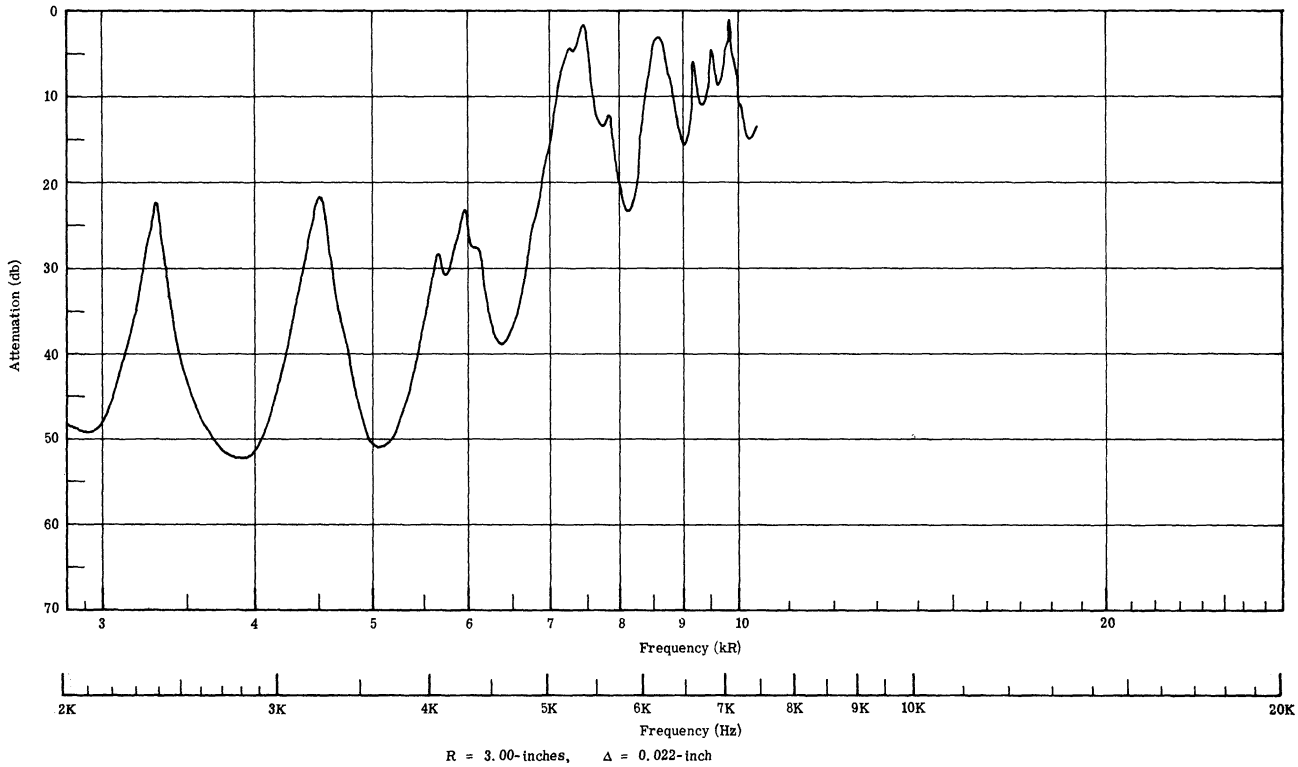

R = 3.00-inches, Δ = 0.022-inch

Fig. 8. Experimental results for copper shell A in air.

when the open end of the probe was located in pressure antinodal regions. At other locations and frequencies, the probe microphone system could not provide useful results even in the case of the 0. 014-inch thick copper shell.

In as much as the larger condenser microphone system was the only one which yielded satisfactory measurements off the normal mode frequencies, the effects of shifting the radial location of its diaphragm were investigated. Figure 9 displays some of the results obtained in this manner. Clearly, the results are dependent upon microphone location across the whole spectrum, but the observed changes are not drastic enough to significantly alter the general interpretation of the interior field at low frequencies.

When the probe microphone was used, the peak at 1500 Hz could be suppressed a little more than illustrated in Fig. 9, but it could not be made to vanish. Even if the diaphragm of the condenser microphone were precisely at the center of the cavity, the lateral extent of the diaphragm would cause it to experience more of the off-axis pressure field than the 1/ 8-inch diameter opening of the probe. Moreover, the lowest signal level at 1500 Hz demonstrated in Fig. 9 occurred when the microphone was located behind center; probably an indication that the mode shape within the spherical shell has been distorted by the bulk of this microphone system.

One additional experiment in air is worth brief mention. From the start of the research we were concerned about how drastically a small leak through the shell would affect the results and whether the presence of such a leak could be recognized from the experimental data alone. That is, a shell with a leak would seem to constitute a form of Helmholtz resonator and a completely extraneous category of phenomenon might be introduced into the experiments. Of course, in the realm of practical engineering applications, a slightly leaky shell might be more realistic than a tightly closed shell.

Among other experiments bearing on such considerations, an experiment was conducted with the 0. 014-inch thick copper shell having a 0. 040-inch diameter hole (No. 60 drill) drilled into it at the equator. Figure 10 shows the results in comparison with results for a closed shell. For the conditions of this experiment, the Helmholtz resonator (fundamental) frequency would be expected to occur far off to the left of the graph at about 45 Hz (calculations based on Eq. 8. 16, Ref. 10). The new broad maximum at about 380 Hz in Fig. 10 probably corresponds to one of the higher modes of Helmholtz resonator action

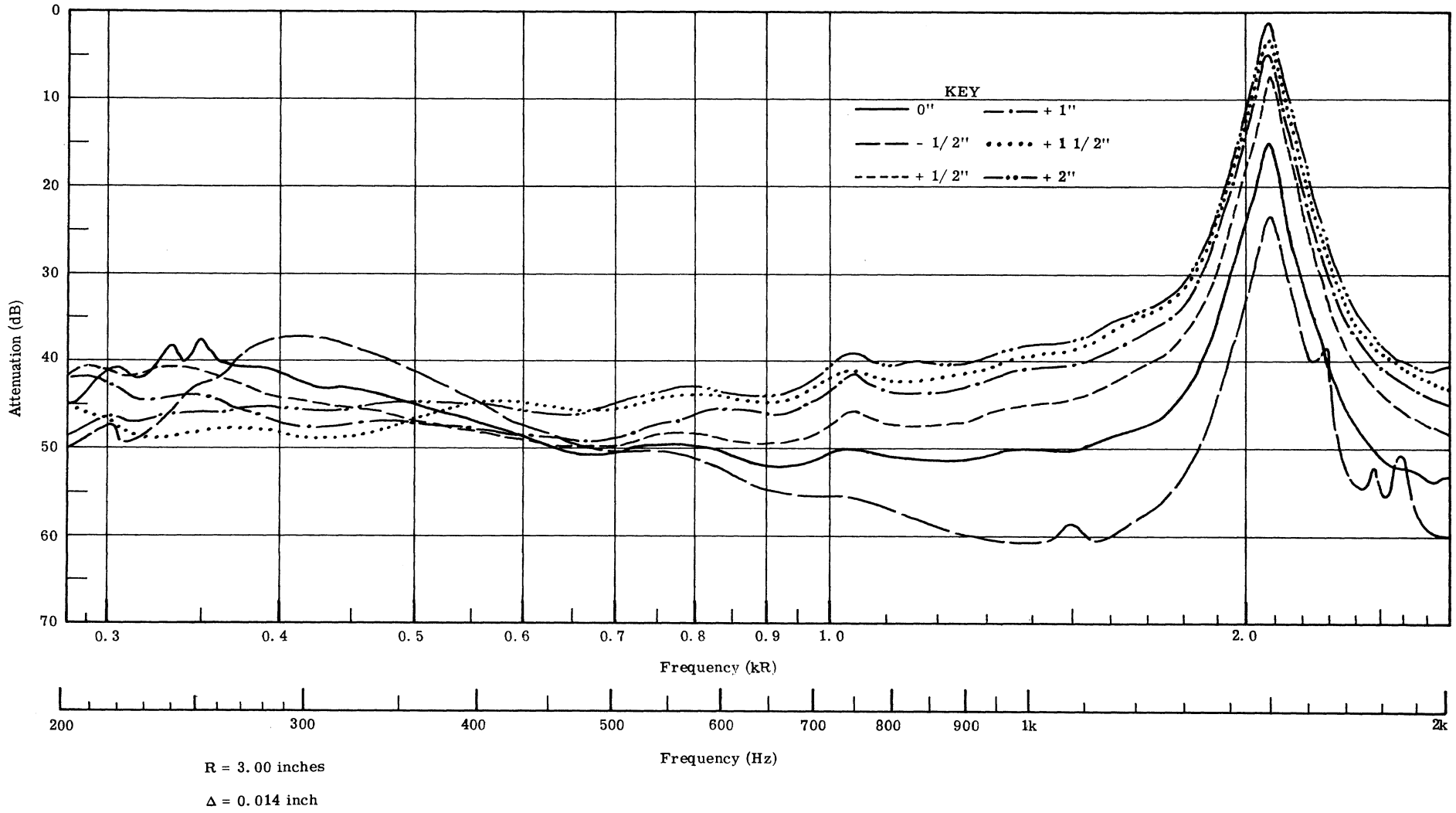

Fig. 9. Variation with Respect to Microphone Diaphragm Location.

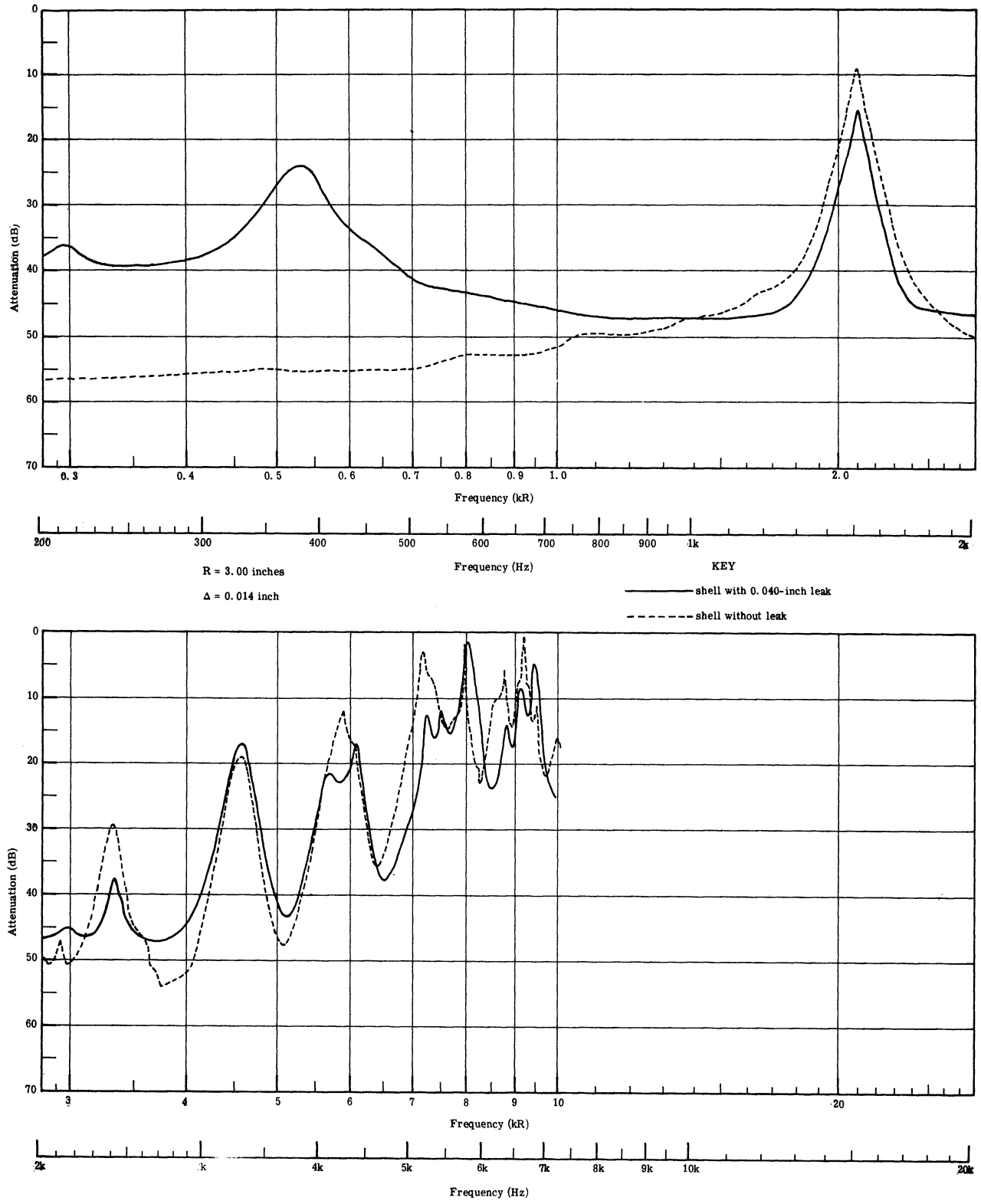

Fig. 10. Effect of a Small Leak Through Shell.

alluded to in Ref. 10. The second mode (for a closed spherical cavity) at about 2440 Hz seems to have been much suppressed by the small leak. Under these experimental conditions, a small leak has changed the results appreciably and precautions against unintentional leaks are clearly indicated if closed-shell results are sought.

3.2 Shells In Air And Filled With Water. This case of different fluids inside and outside of the shell does not seem to have been examined analytically. The analysis in Ref. 3 was general up to the point where the boundary conditions were introduced and then identical fluid media were assumed. Thus, to include different media, it would be necessary to retrace the analysis while keeping track of two sets of fluid parameters in the composition of the coefficients. No mathematical difficulties of fundamental nature should occur; only algebraic complexity. In the case of the scattered field, Ref. 7 comes closer to treating a two fluid problem for in one calculation water surrounded an evacuated spherical shell. In any event, detailed analytical results were not immediately available for comparison with the experimental results related below.

The experimental work on this particular case was motivated by several research needs. It partially decomposed the problem with respect to interior versus exterior measurement problems. It allowed the use of a hydrophone inside the shell without the attendant problems of working completely in water. Techniques of measuring and manipulating the external sound field were identical to those discussed in the previous section. Then, for example, it became possible to consider the effect of an air bubble inside the shell without contending with air bubbles clinging to the outside of the shell.

In the case of a metallic shell in air and filled with air, there is little question that from the inside, the shell behaves like a rigid wall. The shell most definitely does not constitute a pressure-release surface. When the same shell is placed in water and filled with water, the appropriate behavior to assign to the shell as viewed from the inside is not as obvious.

In one instance, we experimented with a shell of acetate plastic whose characteristic impedance was close to that of water and whose shear modulus was low. This shell, filled with water and suspended in air, was expected to behave very much like a sphere of water suspended in air. Its outer surface should constitute a pressure release surface.

If the pressure inside the acetate shell goes to zero at the surface, then the

normal mode frequencies will correspond to the zeros of the spherical Bessel functions. (The zeros in Fig. 6 rather than zero slopes.) The normal modes should be differently ordered than for the previous case of a metallic shell in air and filled with air. Indeed, for the acetate shell in air and filled with water, the sequence should follow the mathematical order of the spherical Bessel functions. Thus the lowest frequency mode would correspond to the first zero of the zeroth-order function and should fall at kR = 3.14 (Fig. 6). For the acetate shell which is 6-15/16 inches in diameter, this should occur at 6850 Hz. The experimental results obtained with this water-filled acetate shell are shown in Fig. 11. Peaks in this curve occur precisely in the order and at the expected frequencies for a sphere of water of this size. Thus the assumption about the physical role of the surface of the water-filled acetate shell is verified. Another point of interest relates to the amplitudes of the normal modes. The simple theory which predicts the mode frequencies does not encompass dissipation hence the experimental values offer the only firm insight on this aspect of the interior field.

Far below the frequency of the lowest mode, the pressure inside the "sphere of water" is practically equal to the acoustic pressure in the air surrounding it. This is as it should be for Pascal's law must govern the behavior. Moving upward in frequency, there occurs a dip, then a rise into the lowest-order mode peak and then successively higher-order mode peaks. Although the conditions attending this experiment were not treated in the guiding analysis, the frequency behavior found in Fig. 11 most closely resembles the analytical predictions. (See Figs. 3 and 4 and also Refs. 3 and 5.) Indeed, one can argue that the resemblance should be expected. In the present experiment, the lowest-order mode is given by the zeroth-order spherical Bessel function and at lower frequencies, this zeroth-order term predominates. Thus it was necessary to go to this unusual (and unrealistic) shell configuration in order to display experimentally an uncontaminated zeroth-order behavior.

This particular transparent acetate shell was useful in other ways. We could see, for example, whether or not bubbles were present on the inner surface of the shell or the hydrophone. Also, when working with the pressure response of a hydrophone in air, the resonant phenomenon (at a normal mode) can be used to enhance the pressure magnitude affecting the transducer; a built-in frequency filter. In Fig. 11, a gain of approximately

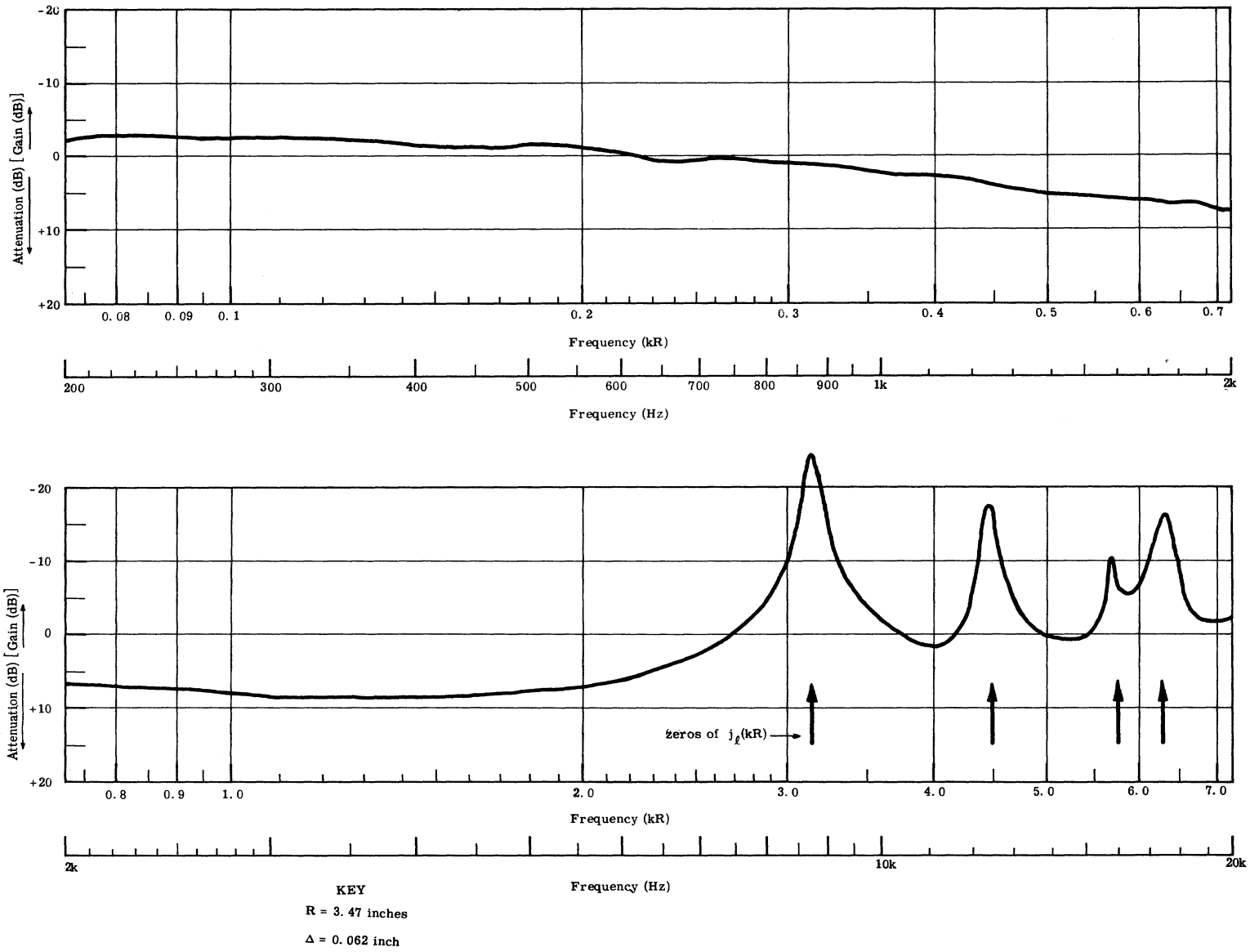

Fig. 11. Experimental Results for Water-Filled Acetate Plastic Shell in Air.

25 db was observed at the lowest nondirectional normal mode.

Several experiments related to the one just discussed were performed with a water-filled plastic bag surrounding the hydrophone. Such a bag has a pendulus geometry which would be difficult to describe in terms of mathematically-simple boundary shapes. Likewise, there is a flat free upper surface to the water. The main consideration is that the bag certainly is very flexible and hence the bag and the free-water surfaces most assuredly constitute pressure release surfaces.

The experimental results were very similar to those shown in Fig. 11. Because the water-filled bag was six or eight inches across and about as deep, the normal modes fell in roughly the same frequency range as for the acetate spherical shell—only here we don't know what geometry to select for calculation of the normal mode frequencies. From the looks of the experimental data, an equivalent-sphere approach would be as good as any.

Figure 12 presents the experimental data for the water-filled plastic bag. In the case of the dashed line, the bag results resemble those for the acetate sphere very closely. The solid line represents the same experimental arrangement after it had been allowed to stand over night. Dissolved air in the water came out of solution and coated the hydrophone and the inside of the bag with a layer of fine bubbles. The effect of these bubbles is evident as low as 1000 Hz and a variety of changes in curve shape have occurred.

This particular experiment with dissolved air had the very limited objective of providing a qualitative indication of what might happen; quantitative investigation was not attempted. It is obvious, however, that such bubble accumulations due to release of dissolved gases might produce some rather startling calibration shifts in free-flooding sonar domes or in any other application where dissolved gases can go in and out of solution during the normal course of operations. Although interference due to bubbles on a hydrophone is a well-known phenomenon, it is rather startling to observe such detailed effects as reproduced in Fig. 12.

Another set of experiments were undertaken with a water-filled, three-liter, round-bottom, pyrex, chemical boiling flask as the shell. Figure 13 illustrates the flask with the hydrophone in position. These experiments were performed subsequently to tests with water-filled metal shells in air and were intended principally to permit visual observation of the interior. The material parameters of pyrex glass (density and the Lamé

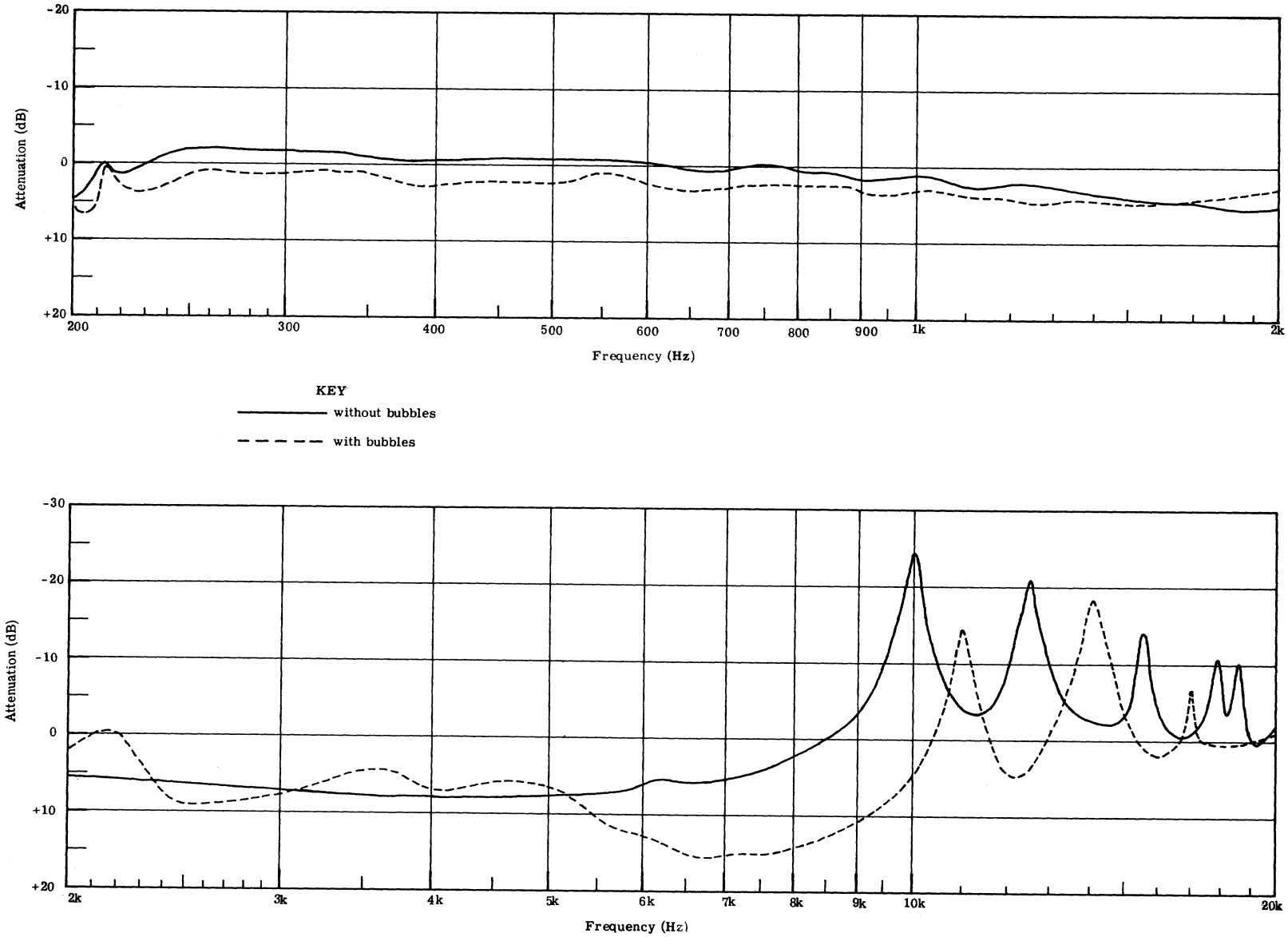

Fig. 12. Experimental Results for Water-Filled Plastic Bag in Air.

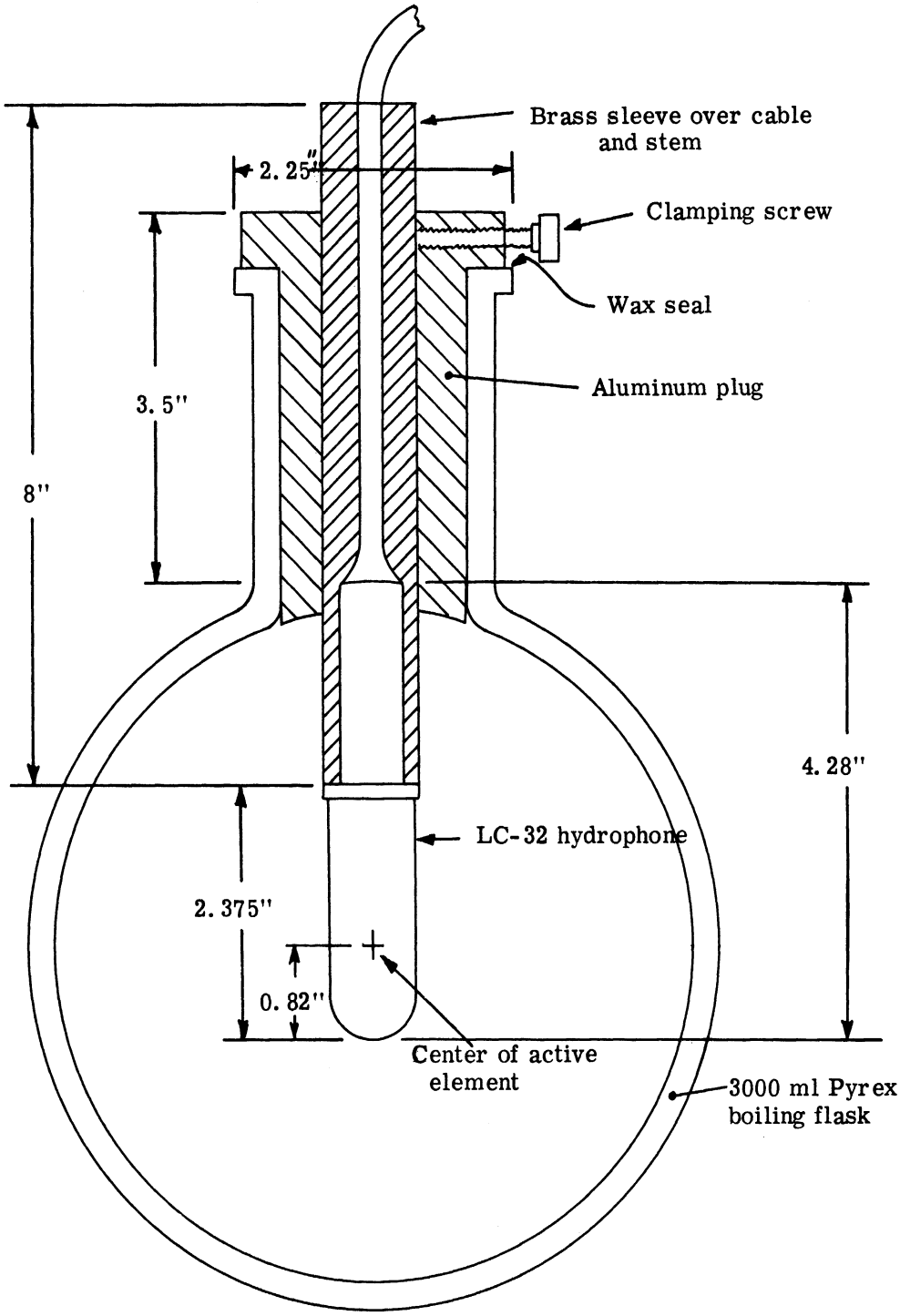

Fig. 13. Sketch of Pyrex Glass Flask With Hydrophone Installed.

constants) resemble those of metal, particularly aluminum, more than they do water or acetate plastic. In this respect, then, the pyrex flask should exhibit a dynamic behavior similar to the metallic shells with the added advantage that the interior could be observed. On the other hand, this chemical flask departed appreciably from an ideal spherical shell by virture of its comparatively large and massive neck construction. As Fig. 13 indicates, this neck was fitted with an aluminum plug so that the internal space occupied by water was very nearly spherical. Nevertheless, the extent of departure of its behavior from that of an ideal spherical shell due both to the neck and plug construction and to the finite size of the hydrophone could not be clearly ascertained. Note also that a brass adapter sleeve has been attached to the hydrophone to allow it to be adjusted in position while maintaining a tight fit in the aluminum plug. The plug was sealed to the glass with beeswax.

As far as the dynamical behavior of the water-filled flask is concerned, it is difficult to decide a priori whether the flask will behave more nearly like a pressure release surface or a rigid wall and the experimental data are not especially helpful on this point either in view of the complex volumetric geometries contributed by the neck of the flask and the hydrophone.

Figure 14 displays typical results from the pyrex flask. The large number of minor peaks above 2500 cps is typical behavior but behavior which is not easily accountable. On the assumption of a pressure release boundary, one would expect to find the lowest normal mode about 8400 Hz or if a rigid boundary at about 5600 Hz and other modes spaced accordingly. In other words, we would expect a similarity to Fig. 11 on the one hand or Figs. 7 and 8 on the other hand. However, these expectations are not fulfilled. When the hydrophone is displaced along its axis from the center of the flask, the general character of Fig. 14 remains although details vary. One situation, see Fig. 15, with the hydrophone placed two inches ahead of center results in a low frequency maximum at about 350 cps which was a repeatable phenomenon at this location although its magnitude was not as stable.

Visible bubbles inside the flask caused some drastic alteration of the spectra as indicated in Fig. 16. Two situations are depicted. In the first case (solid line) the interior of the flask was lined with small bubbles due to natural processes and a moderately large bubble had collected on the underside of the aluminum plug. In the second case (long-dash line) this one large bubble was removed but the coating of small bubbles remained. The most

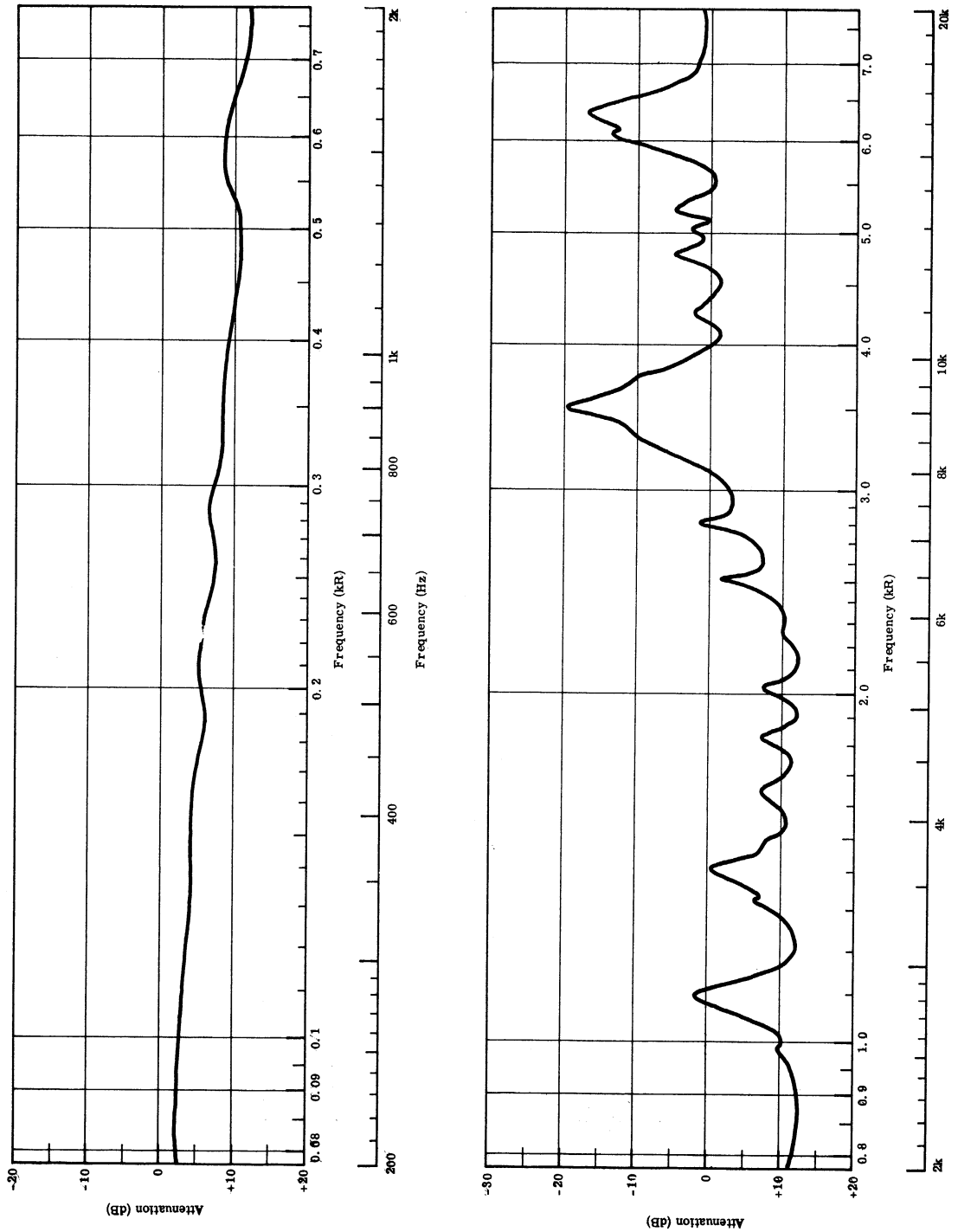

Fig. 14. Experimental Results for Pyrex Flask Hydrophone Centered.

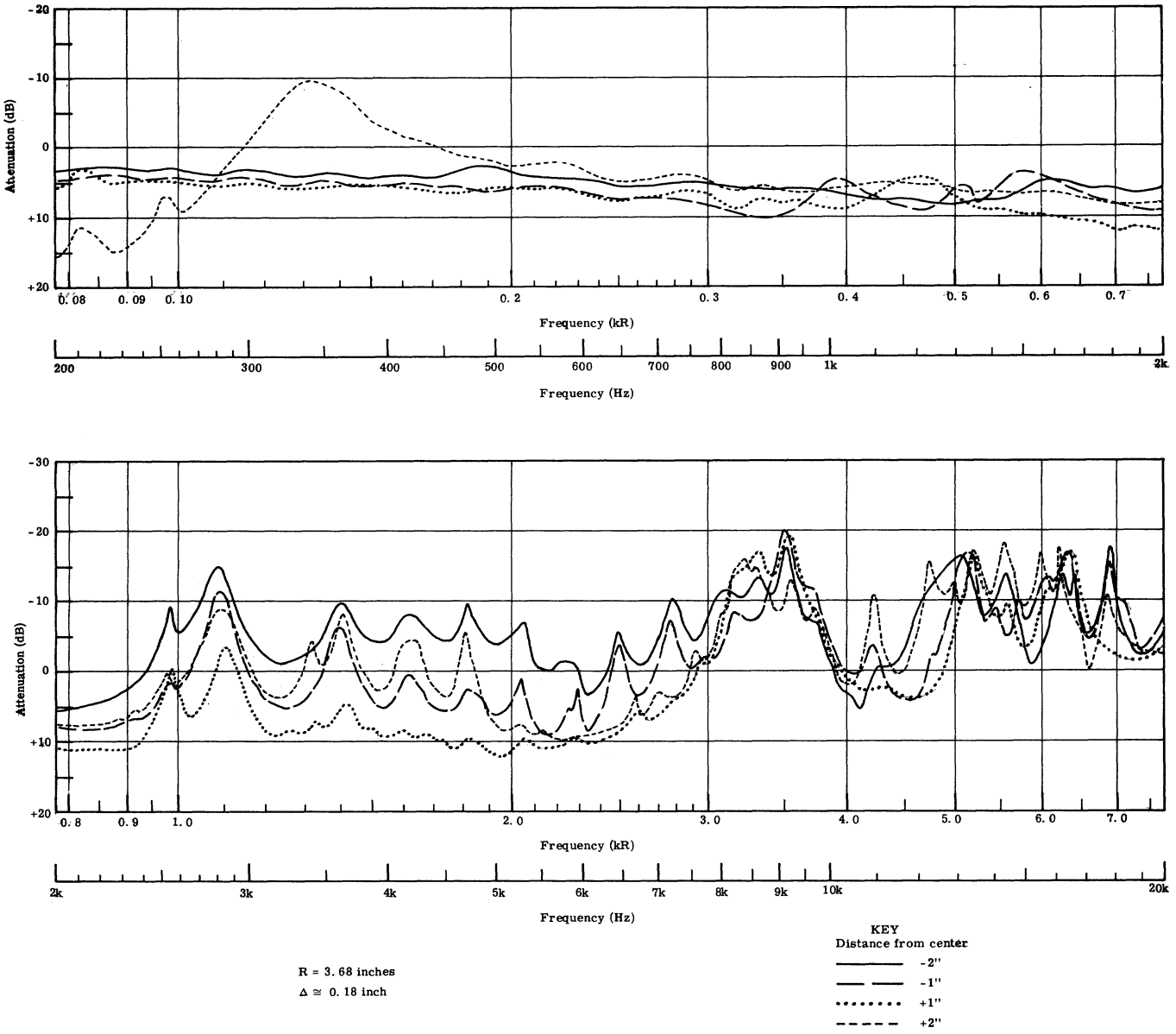

Fig. 15. Experimental Results for Pyrex Flask; Hydrophone Decentered.

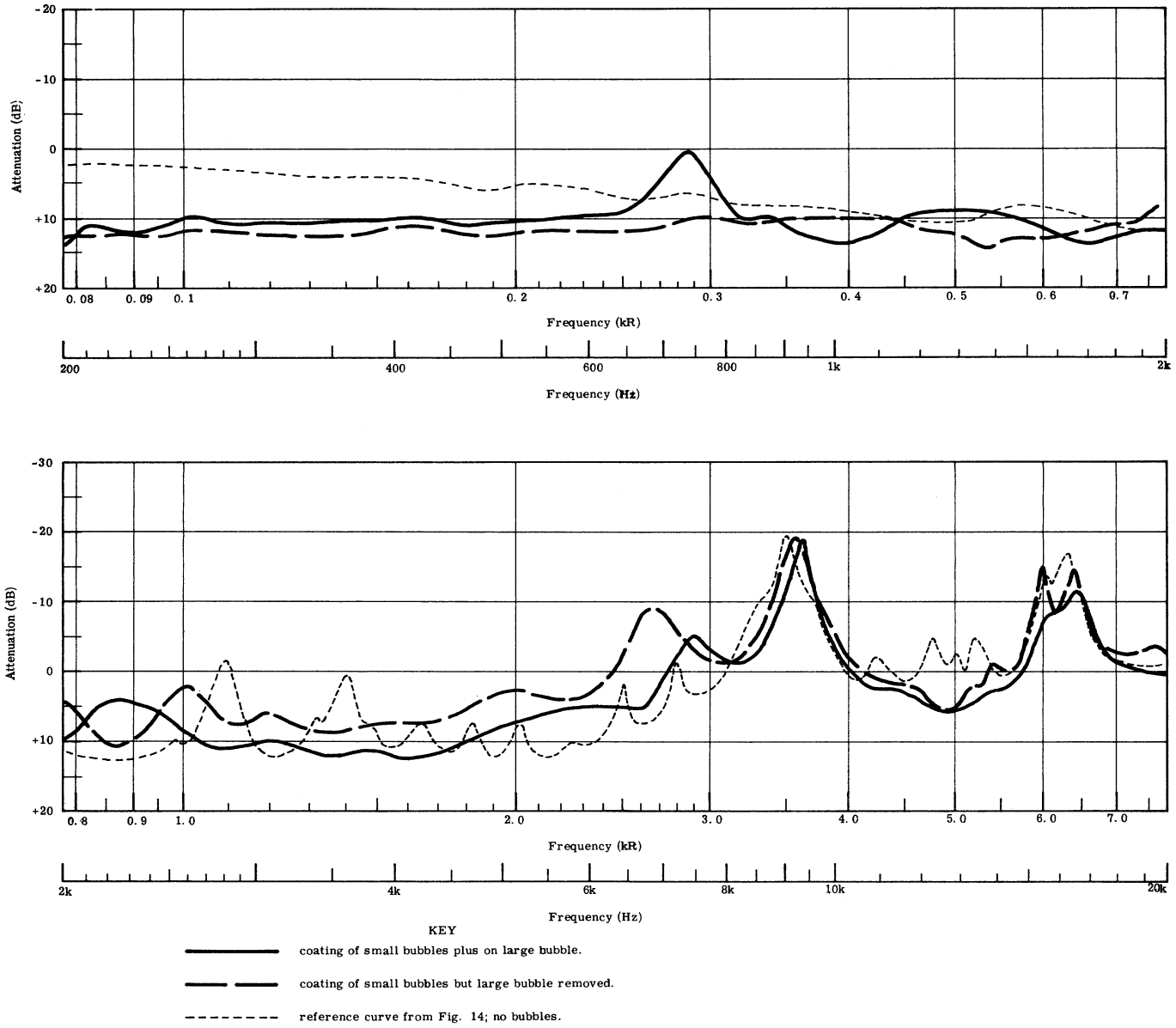

Fig. 16. Effects of Air Bubbles in Pyrex Flask.

obvious consequence of the bubbles (Fig. 16 compared to Fig. 15) is the absence of the many small peaks in the region from 2000 to 15,000 Hz and the general emergence of a cleaner spectrum. Removal of the larger bubble is accompanied by the disappearance of the peaks at 740 Hz and other alterations at higher frequencies.

There is no intention to belabor the interpretation of results obtained with the pyrex flask but simply to employ these observations as a background for considering the results from metallic spherical shells, filled with water and placed in a diffuse airborne sound field. Figures 17, 18, and 19 present such results from two stainless steel shells of different thickness and a third stainless steel shell of smaller radius. The many small peaks between 2000 and 8000 Hz are a prominent feature and, by comparison with the pyrex flask results, suggest that visible bubbles probably were avoided. In order to obtain such results, the water was heated and then allowed to stand several days. The experimental shells were kept filled with such water for weeks at a time, shaken or swabbed to dislodge bubbles, etc. The hydrophone was inserted into the shell with the entire shell immersed in de-aerated water. After the hydrophone was properly positioned, then the shell was removed from the water and its exterior dried. The appearance of the spectra fine structure does not guarantee that the spherical shell was perfectly filled with water. Additional compliance may be present in the form of non-visible bubbles, air trapped in the clearances around the hydrophone insertion fitting or alternatively a small opening here which communicates Helmholtz resonator fashion with the exterior. Likewise, the hydrophone, or parts of it may be more compressible than the water.

In any event, the disregarding the finer structure, Fig. 17 demonstrates peaks at about 8200, 12000, 14,850 and 17,800 Hz for the thinner 8-inch diameter shell. Figure 18 displays a slightly cleaner spectrum and peaks at 8800, 12,500 and 14,600 Hz for the thicker 8-inch diameter shell. The predominately upward shift in frequency may indicate increased stiffness due to the thicker shell but the evidence is not definitive. At low frequencies, the thicker shell seems to consistantly yield a few decibels more attenuation but the magnitude of this difference is small compared to the overall attenuation. Figure 19 shows that for a 6-inch diameter shell, 0.078-inch thick, these modes frequencies lie at about 11,140 Hz and 15,750 Hz. That is, at roughly the same kR values which argues strongly for these modes corresponding to the size and geometry of the shell and not to just fortuitous processes.

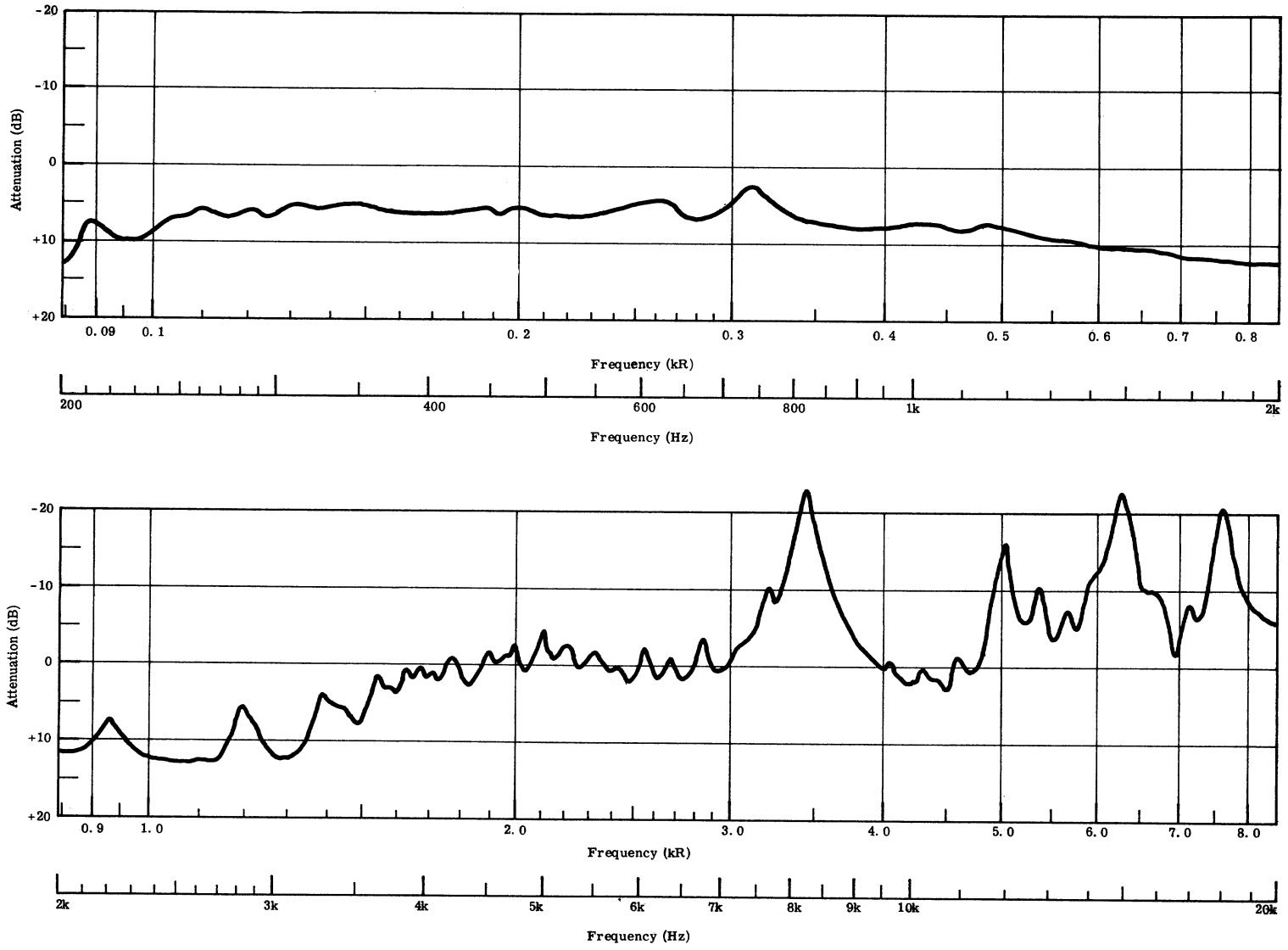

R = 4.00 inches

Δ = 0.037 inch

Fig. 17. Results with Water-Filled Thinest Steel Shell in Air.

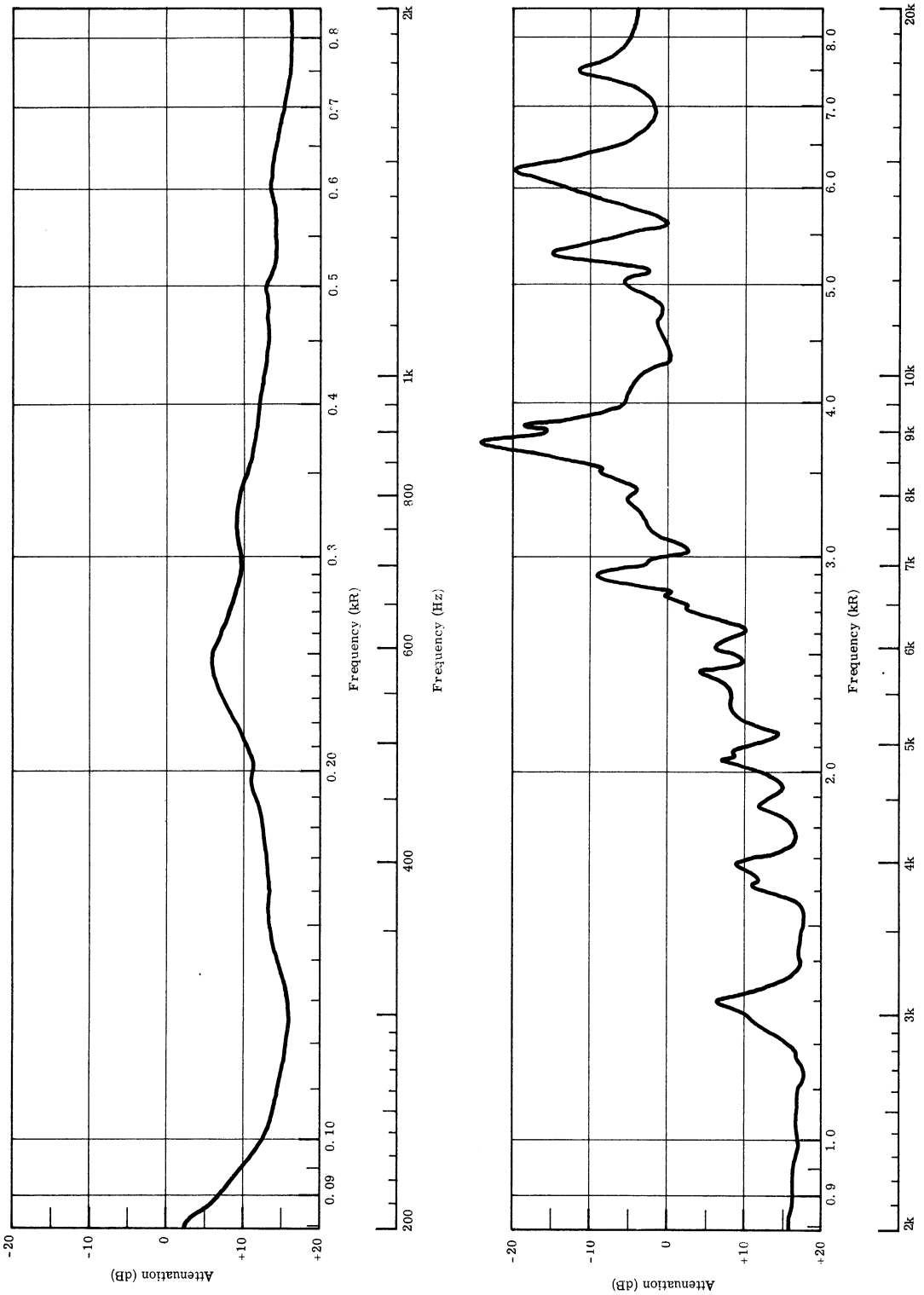

Fig. 18. Results with Water-Filled Thicker Steel Shell in Air.

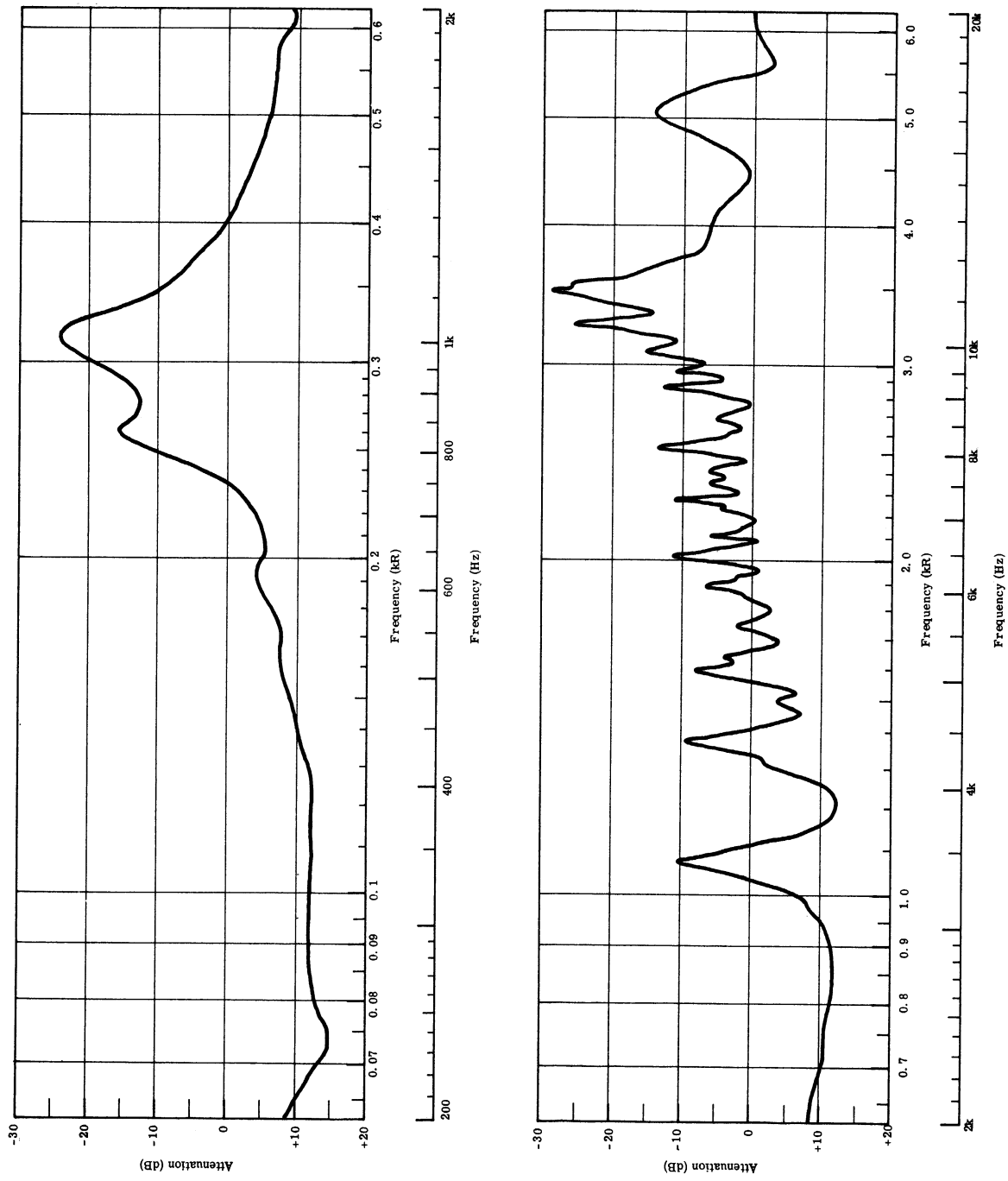

Fig. 19. Results with Smaller Water-Filled Steel Shell in Air.

3.3 Shells In Water And Filled With Water. The underlying theory was addressed principally to this case (Ref. 3) and the initial motivation for the present research was to obtain experimental verification of the analytical predictions. Likewise, the intitial plan of the research was to instrument several spherical shells with hydrophones and to directly measure the sound pressure at the centers of those shells. To this end, a small anechoic water tank (Ref. 11) was constructed to permit laboratory work with instrumented experimental shells. This tank was not expected to be sufficiently free-field to permit the collection of the final definitive data. Consequently the original plan was to test some of the instrumented shells at one of the U. S. Navy's underwater ranges. The purpose of the anechoic tank was principally to assist the development of the preliminary experiments in the laboratory.

As mentioned earlier, the envisioned final data have not been achieved because of various changes in research direction needed to cope with the problems of interpretation of experimental data. It is now realized that a considerably more sophisticated final experiment will be needed than thought originally. Nevertheless, laboratory work with the anechoic tank played a vital role in reaching the current understanding of the problem.

The experiments in the anechoic tank were conducted with a USRL Type J9 source[4] mounted near one end and the shells placed at various distances from the source. In some cases, measurements were performed using one hydrophone with and without a spherical shell. In most cases, however, a second hydrophone was placed outside the shell to simultaneously monitor the pressure in the external sound field. Because of the small values of attenuation expected from the shells, a differential measurement seemed most appropriate in the laboratory and also for the anticipated final tests. In reality, of course, such a differential measurement constituted a comparison involving A_0^I at some external field point and A_0^{III} at the center of the shell and not a direct measurement of A_0^{III} alone. Even so, this type of measurement appeared preferable to the use of a single hydrophone which would have placed extreme demands on absolute calibration of the hydrophone and on the comparatively long-term stability of the entire instrumentation system.

Many tests were conducted in the anechoic tank but most of them are not worth

[4]This source and two model LC-32 hydrophones were borrowed from the U. S. Navy Underwater Sound Reference Laboratory, Orlando, Florida.

reporting in detail at this stage. Some of the difficulties encountered motivated more extensive studies in air of air-filled shells and the water-filled shells already discussed. Other difficulties motivated the extension of the numerical computation discussed in the following section.

One problem related to whether or not air bubbles were present either inside or outside the shell. It appeared essential to be able to recognize from the characteristics of the experimental data alone what condition actually prevailed. Qualified success in this direction was obtained by repeating the measurement several times on different days, each time taking all available precautions such as using de-aerated water, adjusting the hydrophone with the shell submerged, use of a wetting agent on the hydrophone and shell, etc. Of course, the presence of gross bubbles was comparatively easy to recognize but only a sort of asymptotic approach using multiply-repeated experiments offered reasonable assurance of bubble-free data.

As Ref. 11 indicated, the anechoic properties of the water tank did not extend upward in frequency as far as expected. Thus the frequency range available in the laboratory which was reasonably free of standing-wave phenomenon was rather narrow. Tests were made with the monitor hydrophone located at various distances and angles from the shells in order to expand the interpretable frequency range. We were not really successful in this endeavor to correct for residual standing-wave effects although possibly a more elaborate analysis of the spectra would have gained some interpretability. In the main, the anechoic range occurred slightly too low in frequency to exhibit interesting spectral behavior for the small shells being tested.

The analytical model assumed a shell that was free to move and to deflect under the influence of the impinging sound wave while the sound-pressure measurement at the center of the shell should be a point, inertially-fixed measurement. Thus a question existed about how to accomplish the mounting of a shell around a hydrophone in practice. In one set of experiments, a hole was cut in the shell just slightly larger, perhaps 0.015" clearance, than the hydrophone. The hydrophone was clamped firmly to a mounting bracket. The shell was suspended from two thin nylon cords and positioned so that the center of the hydrophone's active area was at the center of the shell. In addition, the shell was manipulated so that it cleared the stem of the hydrophone.

This arrangement caused spectral peaks to occur below 1000 Hz which presumably were Helmholtz-resonator action. Such effects occurred with all shells but were quite variable in details presumably due in large part to variablility in the clearances between the hydrophone stem and the shell. Obviously the shell had to be "sealed" to the hydrophone even though only a few decibels of attenuation were expected. Likewise, such results confirm that the shells constituted relatively rigid containers and presented a significant discontinuity even though the acoustic impedance of the shell material was not drastically different from water. An acetate-plastic shell behaved in similar manner.

As a consequence of the above experiments, a rigid and tighter coupling of the shell and hydrophone was employed. Threaded brass sleeves were soldered to the metal shells or glued to the plastic shells. These sleeves mated with a tight collar which clamped to the hydrophone's stem. In this way the shells were quite rigidly attached to the hydrophone's support bracket and the clearance around the hydrophone's stem reduced to a passage at most one or two thousandths of an inch wide and about 3/8-inch long. This change eliminated the Helmholtz behavior or at least shifted it below the observable frequency range. With this more rigid clamping between the shell and the hydrophone, the only certain compliance was the isolation of the ceramic element from the hydrophone stem within the hydrophone proper. That compliance would provide effective isolation at high frequencies but not at low frequencies and so a discrepancy of unknown importance was introduced between the analytical model and the laboratory model.

The finite size of a hydrophone compared to the shells' radii was another matter of concern. Miniature hydrophones can be constructed but the model LC-32 employed was the smallest convenient "standard" hydrophone. Its radius was about one-tenth of the shell radius and thus might be considered small enough. Further analysis (given in the next section) now confirms that the LC-32 hydrophone was not nearly small enough to permit the observation of pure A_0^{III} behavior in the frequency range employed. Probably an even more serious limitation,however, is the rather large bulk of the hydrophone stem and indeed all of the nonacoustically sensitive bulk. This inert bulk would significantly distort the acoustic field within a spherical shell in a way that would be difficult to correct. Indeed, possibly the only way to observe pure A_0^{III} behavior is to measure at such low frequencies that the zeroth-order term predominates throughout the entire enclosed volume.

Some tests using a thin (0.014" thick, 3" radius) copper shell in water seemed to show some extraneous small peaks between 1000 Hz and 2000 Hz as compared to the stainless-steel shells. The most obvious fault of the copper shell was that its surface was somewhat rippled due to the forming process whereas the stainless steel shells appeared to be perfectly formed. To check on this point, a large dent, about 3" in diameter, was hammered into the copper shell and then it was retested. Figure 20 displays these test results, and the dent seems to have contributed the large excursion at about 900 Hz. Whether this "resonance" is a flexural mode of the dented shell or is related to the shape of the enclosed volume has not been determined.

Figure 21 is typical of some of the better results obtained in the anechoic water tank. The ordinate is the logarithm of the ratio of the interior hydrophone signal to the monitor hydrophone's signal. One of the curves is for these two hydrophones in their respective positions without a shell in place. The various departures from a straight horizontal line are indications of residual standing waves, differentials in the response of the two hydrophones, and possibly other factors. Note that most of the jaggedness occurs above 2000 Hz which fact agrees with the experimental echo reduction reported in Fig. 2, Ref. 11. The frequency range from roughly 1000 Hz to 2000 Hz is particularly clean.

The other curve in Fig. 21 represents the case where a stainless steel shell is mounted over the one hydrophone. Up to about 2000 Hz, the two curves are nearly identical except for the vertical displacement. At higher frequencies complicated changes occur and it is difficult to obtain sufficient precision in frequency to justify a detailed analysis of the differences in order to find the shell's attenuation. If attention is restricted to the frequency range from 200 to 2000 Hz and the average level of the traces obtained (assuming all frequency variation in this range to be artifacts not related to shell attenuation characteristics) then some semblance of reasonableness is obtained. For example, an 8-inch diameter, 0.038-inch thick stainless steel shell gives an average attenuation of 4.75 db while an 8-inch diameter shell, 0.078"-thick yields about 9.75 db attenuation. Such values agree reasonably well with approximate calculations of A_0^{III} which yield 4.9 db and 8.1 db respectively. If anything, this agreement is too good and probably represents the interplay of several fortuitous effects. In the next section, some calculations are given for a steel shell of 24-inch radius and 0.0375-inch thick. The 4-inch radius shells are six

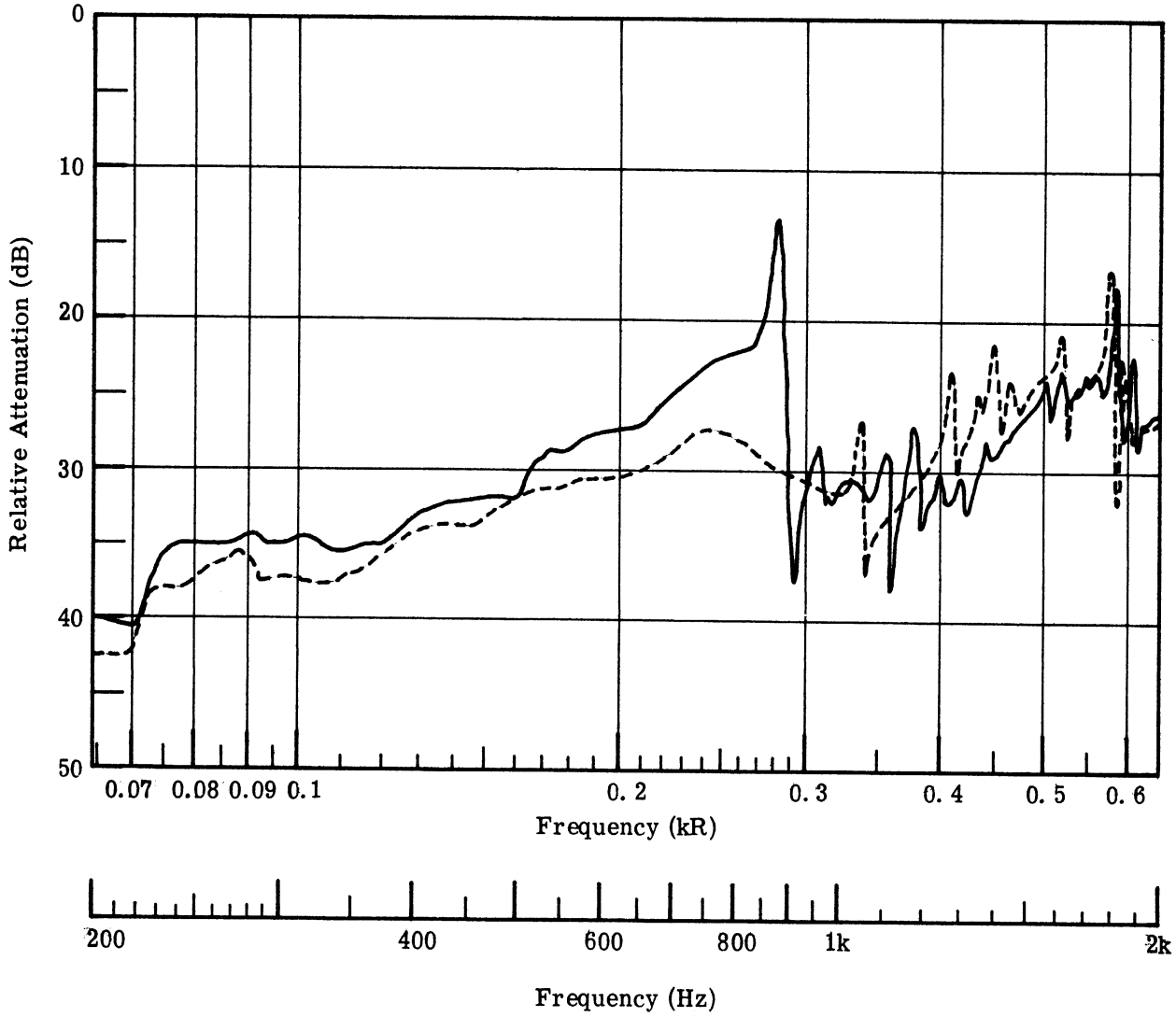

Fig. 20. Results for Dented Copper Shell Immersed in Water.

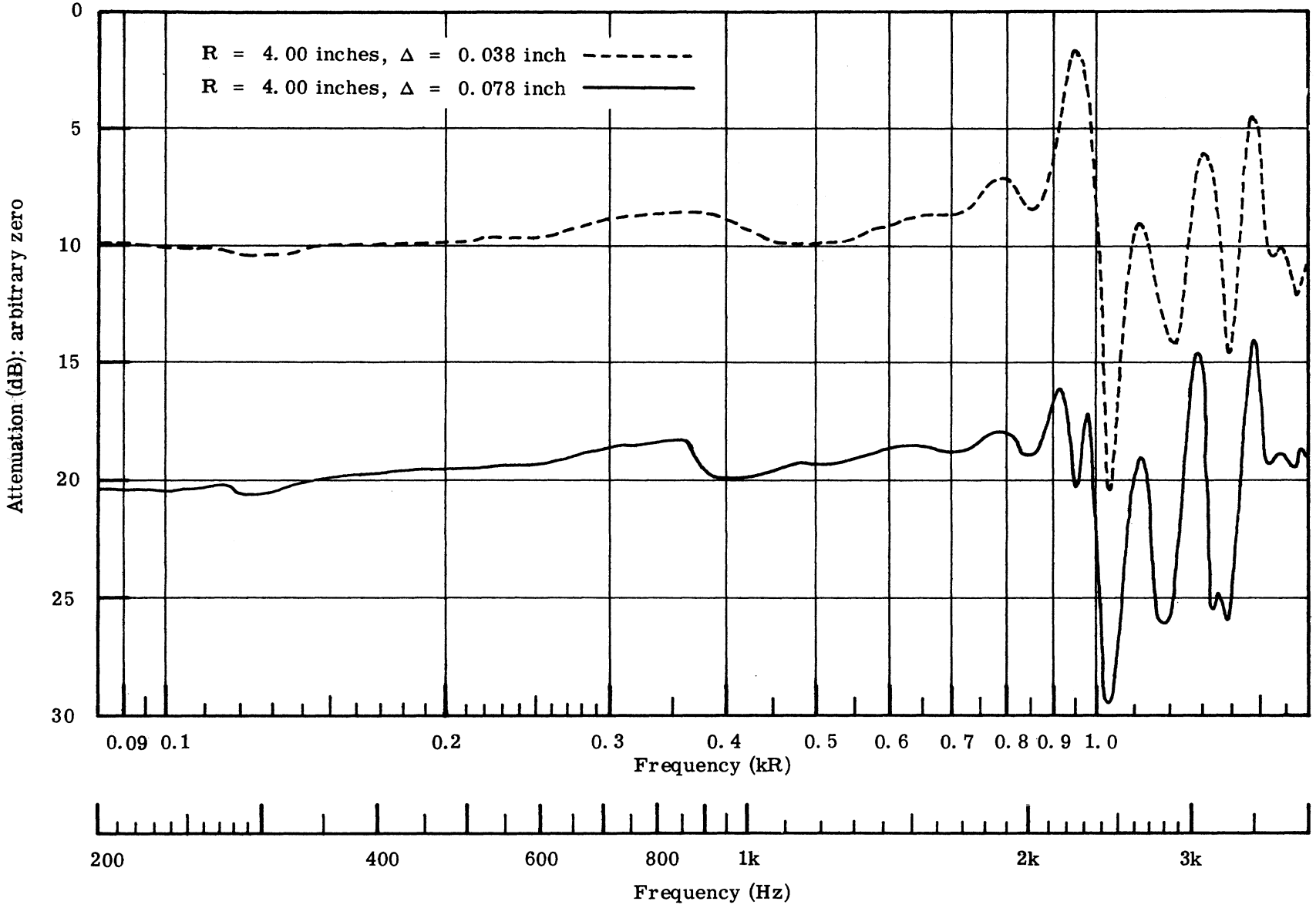

Fig. 21. Results for Stainless-Steel Shells Immersed in Water.

times smaller, thus the corresponding frequencies would be six times higher. Using the same arguments developed there, the A_0^{III} term should predominate throughout the entire interior space below 120 Hz and in a central region of 0. 4-inch radius up to 1200 Hz. Thus the near agreement cited above probably originates from almost operating in conformity with the analysis and the lack of exact agreement is likewise understandable.

Not very much more can be made of the laboratory measurements conducted in the small anechoic tank. They served a valuable purpose in the exploratory stages of this research but the actual data collected remain only indicative, not definitive.

In some experimental pulse studies of scattering from spherical shells of the type described in Ref. 9, it has been observed that the method used to join the two hemispherical shells and the orientation of that equator to the direction of the incident pulse affects the results (Conversation with K. J. Diercks). With respect to the interior fields investigated for this study, no such effects were noticed although the test conditions probably were not critically sensitive to joint construction. In air, both glued and soldered joints were used. The stainless-steel shells were welded together under ordinary production procedures; no special precautions taken. For the low values of argument investigated here, the two criteria for the joint would seem to be:

(a) no large discontinuity in shape or thickness of the shell at the joint, and,

(b) a joint capable of communicating bending stresses across it.

At higher frequencies where vibrational modes of the shell can be expected to play a more prominent role, the joint characteristics may become much more important.

4. EXTENSION OF NUMERICAL EVALUATIONS

During the course of the experimental studies, it became desirable to make certain numerical evaluations for cases not covered previously in Refs. 4 and 5. Various computations were accomplished both on a desk calculator and on a high-speed digital computer. One instance of these additional computations has already been presented in Section 2.1 where A_0^{III} was evaluated for the specific parameters of two copper shells immersed in air.

A troublesome point, which became increasingly important as experimental work proceeded, related to the conditions necessary for the zeroth-order term to preponderate. The guiding analysis had treated the zeroth-order coefficient in considerable detail but not the higher-order coefficients. Thus questions about how high in frequency one may go or how close to the center of the shell one must measure had not been answered in any practical sense.

In order to obtain some insight into such questions, calculations based on the approximate expressions for A_0^{III} and A_1^{III} (Eqs. 3a and 3b) were undertaken. It was assumed that these approximate expressions would be sufficiently precise for the intended purposes; an assumption validated later by computation according to the exact expressions. Initially this assumption was rather shaky because the variation with frequency of A_1^{III} was completely unknown while A_0^{III} was known through Ref. 5.

One of these approximate calculations was undertaken using the physical parameters for sea water and a steel shell 3/8 inch thick and 24 inches in radius. (See Appendix C for numerical values of material parameters.) The same parameter values led to Fig. 2 and the following results were obtained:

$$\left|A_0^{III}\right| \cong 0.44758$$

a value which agrees with Fig. 11 in Ref. 5 and Fig. 2 of this report, and:

$$\left|A_1^{III}\right| \cong 2.4971$$

or

$$\frac{\left|A_1^{III}\right|}{\left|A_0^{III}\right|} \cong 5.6$$

Thus, for this steel shell in water, the approximate value of $\left|A_1^{III}\right|$ is appreciably larger than $\left|A_0^{III}\right|$ and a presumption that the zeroth-order term shall predominate rests heavily on $j_0(kr)$ being sufficiently larger than $j_1(kr)$. Indeed, if the directional characteristics of the higher-order terms are disregarded (and, at most, the Legendre polynomial part of the solution equals unity, see Eq. 1), then for the zeroth-order term to predominate, we might require:

$$\frac{\left|A_1^{III}\right| j_1(kr)}{\left|A_0^{III}\right| j_0(kr)} \leq 0.1$$

and since

$$\lim_{kr \to 0} \frac{j_1(kr)}{j_0(kr)} = \frac{kr}{3}$$

we are led to the conclusion that:

$$kr \leq 0.0536$$

In the present example, therefore, the requirement that the zeroth-order term predominate restricts one to much smaller values of the argument than might be guessed. Often, in the case of problems dependent upon spherical Bessel functions, adequate representation by the zeroth-order term alone can be assumed up to kr-values of 0.5 or even untiy. Not so for the spherical shell problem! The restrictions on (kr) are much more severe.

Continuing with the above line of investigation, we may ask below what value of frequency will the sound pressure measured anywhere inside the spherical shell be controlled

by the zeroth-order coefficient alone? Recall that:

$$kr = \frac{2\pi fr}{c}$$

and solve for frequency with $c = 1.481 \times 10^3$ m/sec and $r = 0.60$m. The answer is 20 Hz. If the region of sound-pressure measurement is restricted to the central one-tenth of the shell's radius, the frequency range may be extended upward to 200 Hz. Examination of Fig. 2 reveals immediately that the most interesting portion of A_0^{III} lies above 200 Hz and that the approximate expression for A_0^{III} is already losing validity. Moreover, the validity of the approximate expression for A_1^{III} remains untested as well as possible significant contributions from still higher-order terms.

A similar calculation was applied to a 3-inch radius copper shell, 0.022-inch thick immersed in air. In this case:

$$\frac{\left|A_1^{III}\right|}{\left|A_0^{III}\right|} \cong \frac{0.29533 \times 10^{-1}}{0.15637 \times 10^{-3}} \cong 1.89 \times 10^{+2}$$

and applying the previous criterion for the zeroth-order term to predominate, namely:

$$\frac{\left|A_1^{III}\right| j_1(kr)}{\left|A_0^{III}\right| j_0(kr)} \leq 0.1$$

we obtain:

$$kr \leq 0.0016$$

In order that the zeroth-order term predominate throughout the entire interior of the shell ($c = 345$ m/sec and $r = 0.0762$m):

$$f \leq 1.15 \text{ Hz}$$

which value is inconveniently low for ordinary experimental acoustical procedures. The microphone used in some of the airborne sound measurements had a diaphragm about one-quarter inch in radius. A parallel calculation requiring that the zeroth-order term predominate over the area of the diaphragm leads to an upper limiting frequency of about 14 Hz;

likewise inconveniently low. In order to work as high as 1000 Hz, the effective diameter of the microphone should be only about 0.007 inch. Evidently, it will be difficult to observe the pure zeroth-order behavior of a shell in air also.

As calculations, such as the approximate ones just cited, loomed larger in attempting to interpret experimental data obtained both in air and in water, it was decided to program for the exact evaluation of at least A_0^{III} and A_1^{III}. Upon expert advice[5], a program was written to solve directly the set of six simultaneous differential equations governing the shell problem rather than to write specific programs to evaluate each coefficient of interest. The printout included all of the coefficients in the analysis by order (A_ℓ^I, A_ℓ^{II}, B_ℓ^{II}, C_ℓ^{II}, D_ℓ^{II}, and A_ℓ^{III} in the notation of Ref. 4) although only the A_ℓ^{III} were of immediate interest.

The usual difficulties in obtaining "correct" results were encountered and the computational effort became an on and off affair depending inversely upon how the experimental work seemed to progress. At one point, computational effort was completely discontinued when apparently wild results were obtained. Later it was discovered that a routine, borrowed from another application, was producing a transposed solution which had been acceptable in its original application because of the symmetry of the governing equations, the transposed solutions appeared as nonsense. Once this difficulty became known, it was a comparatively simple task to correct the spherical shell program and to obtain what now appear to be correct solutions. This final adjustment to the computer program occurred near the end of the active contract period and so only a few calculations were run.

These final calculations appear to be correct in as much as the values of A_0^{III} agree with those published in Ref. 5 which in turn were produced by a straight-forward evaluation of Eq. 2b. The newly calculated values of A_0^{III} agree with those mentioned in the footnote on page 14to four significant digits and a comparison with one of Hickling's (Ref. 7) values for the scattered field agreed within about two percent (Appendix B). Nevertheless, several doubts linger including the algebraic sign of certain terms, the precision of the

---

[5]This program and all digital computations were performed by the Computation Department, Institute of Science and Technology, The University of Michigan using an IBM-7090 computer. The assistance of Mr. John Riordan, Research Mathematician and head of the Computation Department, is gratefully acknowledged.

answers, and the range of argument accommodated without recourse to special procedures. Basically, the final program should permit numerical investigation of the effects of parameter variations on the acoustical fields both inside and outside of the shell in an efficient manner. Nevertheless, because the computer results are so difficult to verify, a very thorough recheck of the program ought to preceed any elaborate use of this program. As an example of the computation time required by the present program, it produced a printout of five significant digits of the real and imaginary parts of all six coefficients (A_ℓ^I, A_ℓ^{II}, B_ℓ^{II}, C_ℓ^{II}, D_ℓ^{II}, A_ℓ^{III}) for five orders ($\ell = 0, 1, 2, 3, 4$) for 18 different frequencies for two different shells in an elapsed time of 1' 19. 1".

Figures 22 and 23 present these computed results graphically for a steel shell in water and a copper shell in air respectively. In both figures, the magnitude of the coefficient A_1^{III} is larger than A_0^{III} and rises to a peak at a lower frequency than A_0^{III}. For the steel shell in water (Fig. 22), the difference at low frequencies is 15 db, an answer consistent with the approximate calculations given earlier in this section. Now, however, the general frequency dependence of A_1^{III} is known (assuming that the computer program is correct) and the earlier approximate calculations are seen to be appropriate to frequencies as high as several hundred cycles per second. ($kR \cong 0.5$ to 1.0). The earlier comment about being limited to extremely low frequencies if pure A_0^{III} behavior is to be observed experimentally is valid likewise. In addition, it is observed that when sweeping upward in frequency, significant variations appear in the first-order coefficient before anything interesting occurs in the zeroth-order coefficient. This fact limits observation to an even smaller region precisely at the center of the shell if the interesting frequency dependence of the pure zeroth-order coefficient is to be observed experimentally. In almost any practical situation, experimental observations would be predominated by the first-order coefficient or possibly by even higher-order coefficients. Figure 22 indicates that A_2^{III} rises to larger values and at lower frequencies than either A_0^{III} or A_1^{III}. Of course, because of the nature of $j_2(kr)$, this second-order term is more easily suppressed by operating at small values of (kr) than A_1^{III} but at values of say $kr \geq 1.0$, its contribution probably must be taken into consideration. (Incidentally, reservations about the accuracy of the present computer program cast more doubt on the higher-order coefficients so not too much point is made of them here.)

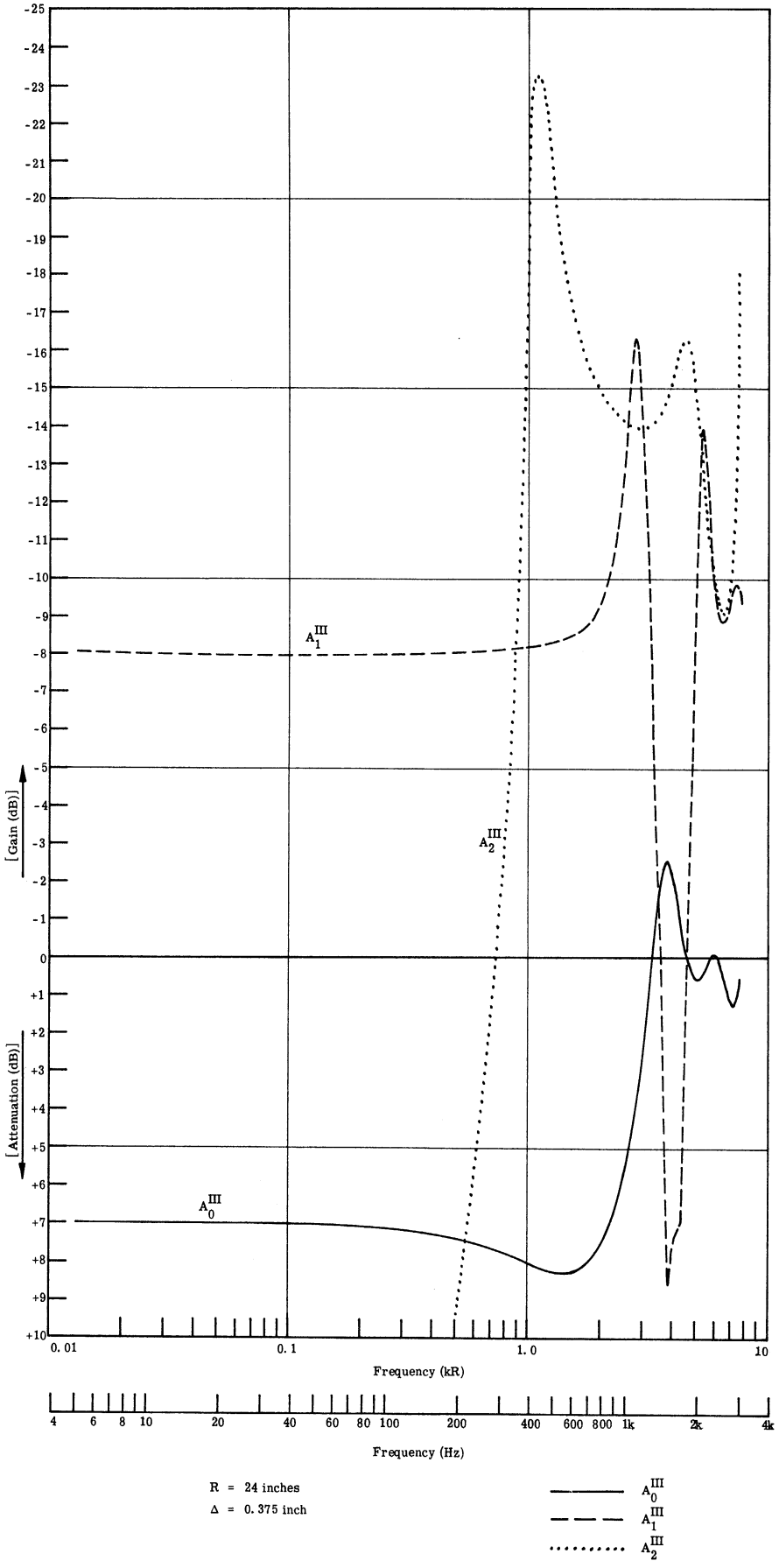

Fig. 22. Computed Coefficients for Steel Shell Immersed in Water.

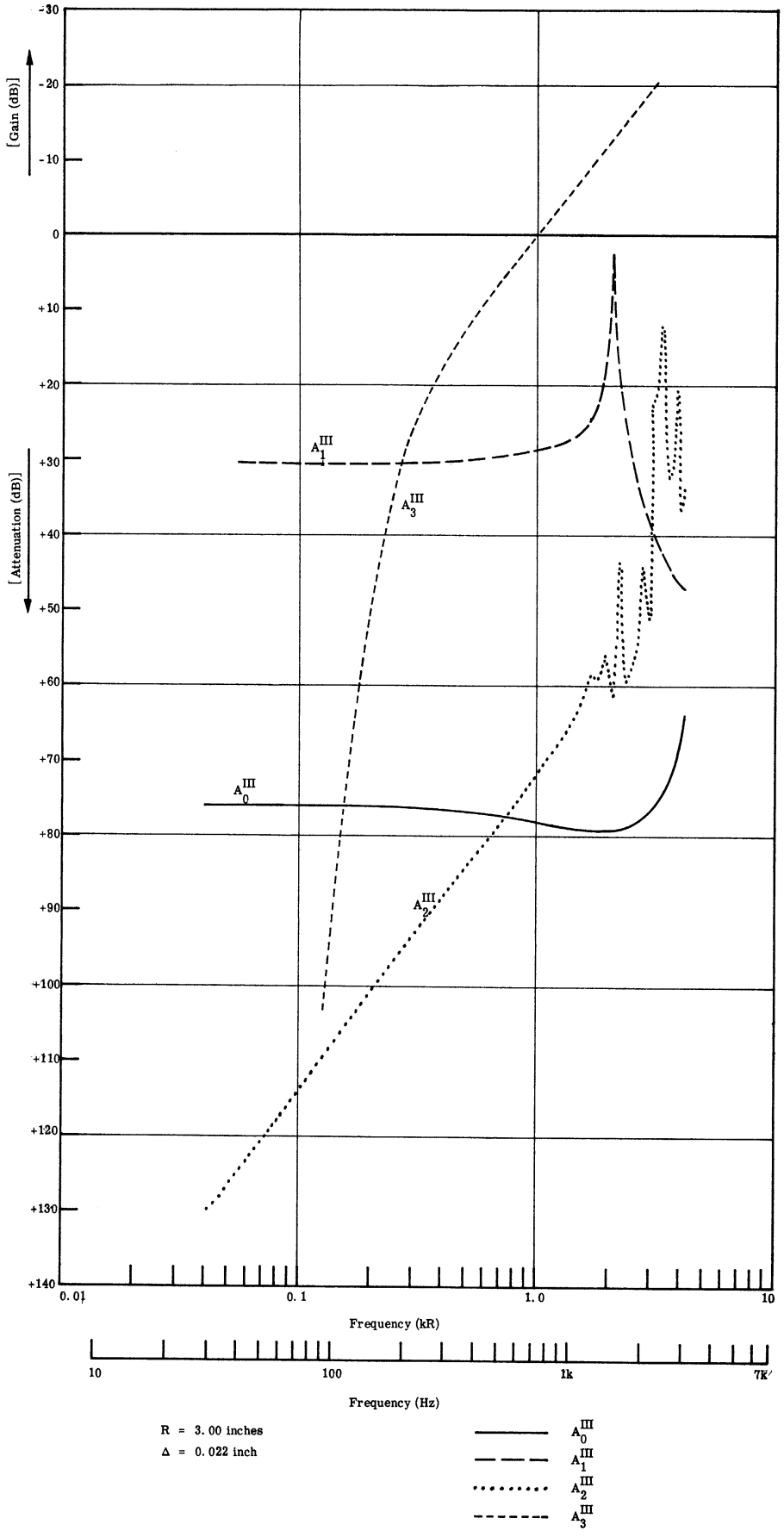

Fig. 23. Computed Coefficients for Copper Shells Immersed in Air.

Refering to Fig. 23, a very similar situation is found for a copper shell in air. At low frequencies, A_1^{III} is 35 db larger than A_0^{III} which is a tremendous magnitude to suppress by operating at low values of the argument. Likewise, A_1^{III} peaks at lower frequencies than A_0^{III} and there is indication that the higher-order coefficients possess significant magnitudes at comparatively low frequencies also.

At very low frequencies, the final computer program gives slightly erratic results. For example, the values of A_0^{III} and A_1^{III} begin to deviate from the steady values displayed in Figs. 22 and 23 and also from the lower limiting values computed on the basis of Eqs. 3a and 3b. Such erratic computation should be expected due to truncating of the functions involved. A modified computer program would be needed to successfully approach an argument of zero. As the program now stands, the first two coefficients settle down to their appropriate values when kR is about 0.02 or larger. Likewise, the computed values of say A_3^{III} produce somewhat jagged graphs even within the range of argument where A_0^{III} and A_1^{III} and possibly even A_2^{III} yield smoothly varying graphs. This behavior also is thought to arise from insufficient accuracy at points within the computational procedure. However, it should be possible to obtain several more of the higher-order coefficients in a straight forward manner without resorting to special computational routines. Up to this stage, the computer printout has been in terms of the coefficients but simple extensions of the program could print out a complete solution for Eq. 1 for a specified field point and angle to match any desired experimental configuration.

By examining Figs. 22 and 23, and estimating how these would alter when the coefficients are multiplied by the appropriate $j_\ell(kr)$ value, one can obtain an idea of how the sound pressure fields inside the shells vary. It was noted previously that A_1^{III} peaked at a lower frequency than A_0^{III}. The relative contribution of these two orders varies according to the location selected for the internal field point. If we consider a point at the interior wall of the shell, i.e., $j_1[k(R-\Delta)]$ goes through its first maximum at a slightly higher frequency than $j_1(kR)$ but not enough higher to appreciably alter the estimates unless rather thick shells are considered. As the computations stand, both for a metallic shell in water and in air, the closest elementary cavity would seem to be the rigid cavity; not a pressure release surface. It follows then that the observed ordering of normal modes ought

to correspond to the zeros of $\frac{dj_\ell(kr)}{d(kr)}$ rather than of $j_\ell(kr)$; at least for the first several modes. Since the spherical shell indeed is not perfectly rigid, the particle velocity viewed from the inside is not precisely zero at $r = R - \Delta$ but will have fallen to a small value. In this sense, the mode behavior at low-frequencies and / or low-order modes resembles that for a rigid spherical cavity of slightly larger radius.

On the basis of the above picture of modal distribution for the low-order modes, if one does not perform a point measurement precisely at the center of the shell, he should first encounter a peak due to the first-order term, next the second-order term and then one due to the zeroth-order term; the order of derivative zeros in Fig. 6 neglecting the one from $j_0(kr)$ at zero frequency. Such an ordering agrees completely with the experimental results obtained in air. It probably should be expected for a shell in water also when a sufficiently good experimental measurement is obtained. Likely the magnitude of the intensity variations to be observed in water will be relatively small. Presumably, even a lucite shell in water should behave more like a rigid cavity than like a pressure-release surface but this speculation needs confirmation from additional computations and / or experiments. It would appear to be theoretically possible to select parameters for a "shell material" in water which would be pressure-release like in the ordering of normal modes in the interior space. It might even be possible to fabricate an experimental shell exhibiting such behavior from perhaps foamed rubber or foamed plastic for example.

The extended numerical evaluations lead to an understanding which correlates closely with physical intuition. Recall that the low-frequency approximation of A_0^{III} (Eq. 3a) is essentially a stiffness-dependent coefficient since it did not contain density terms. At extremely low frequencies, stiffness must predominate and the analysis confirms this. However, before any significant frequency variation is encountered, density reappears as a significant parameter for all realistic measurements inside the spherical enclosure. Only a point measurement performed precisely at the center of the shell can preserve a zeroth-order term preponderance and thereby isolate density from the Lamé constants of the material. Under more normal circumstances, the acoustical attenuation of a shell is related to the mutual effects of the several material parameters.

Limited consideration was given to the question of whether Eq. 1 at high frequencies yielded the same predictions as Eq. 6. By considering the form of the asymptotic

expressions for the spherical Bessel functions of large argument, one can almost see something closely related to Eq. 6 emerging. However, no completely satisfactory mathematic equivalence was obtained during the time devoted to this consideration. Physically, for a large enough shell and high enough frequency, an interpretable correspondence must exist.

A different point arises at low frequencies. The layered-media concept as embodied in Eq. 6 is often assumed as a first approximation even at low frequencies. In the case of a closed spherical shell, enough is known to be certain that Eq. 6 is not an even remotely appropriate expression. When it was thought that A_0^{III} embodied all of the essential low-frequency behavior, the different parametrical dependence was very marked indeed. Now that it is realized that density enters prominently and at relatively low frequencies also by way of A_1^{III}, the situation is not quite as clear cut. One might guess that the combined effects of the A_0^{III} and A_1^{III} coefficients do not yield the same dependence as predicted by Eq. 6 but just how strongly they disagree and to how high a frequency one must go to obtain essential agreement remains an open question.

5. SUMMARY AND RECOMMENDATIONS

The investigation of sound transmission through spherical shells originally reported in Refs. 4 and 5 (and condensed for the open literature, Ref. 3) has been extended with numerical analysis and experimental studies both in air and in water. The theoretical investigation had indicated that at low frequencies a considerably different relationship held between a shell's material parameters and its acoustical attenuation than would be expected on the basis of characteristic impedances and the usual layered-media considerations. The exact analytical relationships for a spherical shell are complicated, but at low frequencies and near the center of a shell, considerable simplification can be invoked.

The original analysis indicated that at the center of a shell and at low enough frequencies, the zeroth-order solution alone was sufficient. Mathematically, this is correct but further investigation has demonstrated that the conditions necessary for the zeroth-order solution to predominate are much more restrictive than thought initially. Thus for practical shell structures, even under laboratory conditions, pure zeroth-order behavior is almost impossible to achieve. This result has been demonstrated both analytically and experimentally.

Thus, for practical shell structures both in air and in water, account must generally be taken of at least the zeroth-order and the first-order terms and possibly in some cases of even higher-order terms. That this is true derives from a combination of two considerations. For real shell materials, particularly metals, the first-order coefficient at low frequencies is numerically much larger than the zeroth-order coefficient. In addition, the radial dependence of the first-order solution, namely $j_1(kr)$, approaches zero for small values of argument comparatively slowly and hence it can not easily suppress its numerically large coefficient. Terms of second- and higher-orders appear to be sufficiently suppressed to be disregarded in low-frequency investigations although more work is needed to clearly establish the limitations. Obviously, at high frequencies the spherical shell model should yield results in agreement with the usual layered media predictions but this too remains to be demonstrated formally.

In addition to purely mathematical considerations, the finite dimensions of practical microphones or hydrophones placed inside a spherical shell seem to distort the internal acoustical field. Thus the suppression of first- and higher-order terms near the center of a shell expected on a mathematical basis is not achieved. It would appear that only a remote measurement of the internal sound pressure field, say by optical means through a transparent shell, could achieve the analytically predicted results. In practical applications of a spherical shell such as in a sonar dome, the large hydrophone structure would undoubtedly cause more extreme divergence from the analytical behavior than for the laboratory experiments reported here.

Laboratory experiments with small spherical shells immersed in air exhibit a normal mode sequence closely resembling the normal modes for a rigid air-filled spherical cavity of the same dimensions. The lowest-frequency mode corresponds to the first, not the zeroth-, order solution and falls at an argument value of about 2.1. The third lowest mode is the first one attributable to the zeroth-order solution. At frequencies well below the lowest mode, the attenuation caused by a thin spherical shell is very large although practically not as large as would be expected from a consideration of A_0^{III} alone. It is possible, however, to achieve 55 db attenuation below 1000 Hz through 0.014-inch thick copper in the form of a six-inch diameter shell. Thus the spherical shell constitutes one approach to creating a very quiet space with a light-weight stiff structure if one is content to operate below the first cavity-mode frequency. At the mode frequencies themselves, such a shell exhibits little attenuation, at least when the interior is devoid of acoustical absorption. The observed low-frequency attenuation is so large that small air leaks or acoustical shorts cause large changes and any sizable leak converts the shell into a Helmholtz resonator.

The case of different fluids inside and outside of a shell was not treated explicitly in the original analysis although it can be accommodated with some additional algebraic complexity. Several experiments in this configuration were performed in the laboratory using water-filled shells in an airborne sound field. A thin acetate-plastic shell acted as a pressure-release surface bounding a spherical body of water. In this situation, the observed internal modes followed the mathematical ordering of the spherical Bessel functions, the lowest frequency mode corresponding to the zeroth-order term, etc.

Experiments in air with a water filled pyrex-glass flask were used to investigate

the effects of bubbles in the enclosed space. The absence of bubbles is accompanied by a multitude of small peaks lying below the lowest cavity mode encountered. The detailed origin of these peaks is unresolved. Water-filled metallic shells tested in air gave similar results in as much as similar small peaks were most evident when presumably bubble-free conditions existed on the interior of the shell.

Experiments with metallic shells immersed in water were more valuable in clarifying general interpretation than providing specific validation of the analysis. The anechoic frequency range of the laboratory tank was too narrow to encompass the lowest-frequency modes of the experimental shells and residual standing-wave effects made detailed quantitative analysis difficult.

Even small clearances between a shell and the penetrating hydrophone stem result in pronounced Helmholtz resonator action in water. This result indicates that the shell is stiff enough to constitute a water-filled cavity. The spherical-shell behavior when immersed in water appears very dependent upon exact spherical geometry in as much as deliberately denting a copper shell introduced some pronounced excursions at frequencies well below the lowest spherical-cavity mode.

The measurements, in the laboratory, on metallic and plastic shells immersed in water confirm the analytical predictions with respect to the general magnitude of low-frequency attenuation. They also confirm the need for simultaneous differential measurements if accurate comparisons are to be made between theory and experiment.

Further numerical analysis has clarified the nature of the low-frequency attenuation through a spherical shell. Both in air and in water, a metallic shell behaves more like a rigid cavity than a soft pressure-release surface. Dominance of the zeroth-order coefficient can only be maintained very close to the center of the shell and at very low frequencies (actually, at very small values of argument). The first-order coefficient for metallic shells is larger at low frequencies than the zeroth-order coefficient and it is difficult to suppress simply by working at small values of argument. Even under laboratory conditions, it is usual to observe effects due to the first-order term. Furthermore, the first-order coefficient shows interesting frequency behavior at lower frequencies than the zeroth-order term.

A computer program was developed which supplies all of the coefficients for the spherical shell problem up through several mathematical orders. So far, it has been used

only to provide predictions for two experimental shells but it appears capable of facilitating a much more thorough and extensive investigation.

Additional effort will be needed to complete the problem. The analysis of an immersed spherical shell has introduced an important and complicated problem with overtones of pure acoustical physics and practical acoustical engineering. In addition to acoustical impedance considerations of sound transmission through layered media (implicit but obscured by the algebraic complexity attending the spherical geometry) there are included the modal behavior characteristic of a spherical cavity and the vibrational behavior characteristic of a spherical shell. As yet, these physically important limiting cases have not been clearly demonstrated analytically.

A satisfactory computer program for direct solution of the set of six simultaneous partial differential equations appears to have been achieved. Separate identities for the exterior and interior fluids were maintained but this feature has not yet been utilized in the printout. A thorough investigation of the range of applicability of the program is needed before attempting to fully exploit it. The output for very small values of argument is known to become incorrect due to truncation errors and special computational procedures would be needed to approach a zero-value argument in the limit. This deficiency for very small argument is not of serious import however because appropriate algebraic expressions exist for A_0^{III} and A_1^{III} and they can be used to identify divergence of the computer output at small argument.

It remains crucial, however, to determine how the program functions at relatively large values of argument and for high-order terms. There are suspicions that truncation errors may cause trouble in these cases also but so far no clear or independent check has been applied.

After the range of applicability has been determined (and extended by revised procedures if found wanting) we will be in a position to explore a variety of important questions numerically. It should not be difficult to extend the program to provide specific values, order by order, for specific field points both inside and outside the shell or to take the ratio of these as might be needed for comparison with specific experimental data. Likewise it should be possible to sum over as many orders as necessary to achieve adequate precision in an answer. (At high frequencies, convergence becomes slow but Hickling,

Ref. 7 has worked to relatively high orders with the scattered field without encountering serious limitations.) Also it should be possible to include the angular variation to accommodate either the directionality attendant to plane-wave situations or to integrate with respect to angle for diffuse-field situations.

Therefore, one should be able to investigate numerically all of the interesting cases of varying the parameters of the spherical shell problem at low and medium frequencies. And it is at low and medium frequencies where the spherical-shell problem promises the most new information.

The parameters for real materials and representative shell dimensions can be entered in an extension of the approach used by Miss Stern in Ref. 5. However, at this stage, it might be more informative to depart from the parameter values representing real materials and to increment parameter values to clearly display the role of each independently

An important extension of the problem would be the use of different fluids inside and outside of a shell. There might be significant advantages to certain combinations. In geometrical optical problems one usually deals with the short-wavelength approximations while the present spherical shell problem is more closely identified with a long-wavelength approximation. Nevertheless, in optics, the sensitivity gain for an immersed detector is well-known and there may be equivalent acoustical advantages. Likewise in optics, there are considerations such as the spherical aberration introduced by a dome, the optical power of a dome, the use of quarter-wave layers to reduce reflection losses, etc. Somewhat weaker but nevertheless significant acoustical effects may appear now that we are in a position to make the requisite calculations. Even if significant effects fail to materialize at the lowest frequencies, something ought to begin to appear at medium frequencies. After all, acoustic lens effects become evident when an aperture is only a few wavelengths across and sonar dome spoking occurs where diffraction effects would ordinarily be considered negligible.

Additional unguided experiments with spherical shells would seem to be of small value at this stage. Much of what has been learned in the present research has been due to interaction between theory and experiment. However, we are now in a position to accomplish a more detailed analysis than previously and new experiments guided by such analysis would be most appropriate. The complete interior acoustical field should be predicted for

specific shells up through several mathematical orders along with the corresponding field at the location of an external monitor transducer. The appropriate experimental data can then be collected with essentially complete a priori knowledge of what to expect if the experiment proceeds properly and also an idea of the form of probable deviations.

The use of larger ratio of shell radius to transducer radius would aid in observing pure A_0^{III} behavior. However, even then one can probably only observe the lowest-frequency horizontal portion of A_0^{III}, that is, the limiting low-frequency magnitude. Interesting frequency behavior would almost certainly involve contributions from several orders.

The present experiments indicate that the entire interior transducer bulk ought to be centrally located. The microphone's preamplifier or the hydrophone's stem distort the acoustic field within a shell causing a loss of suppression of the higher-order terms. In order to minimize this effect, the transducer's bulk ought to be small and roughly sperical in shape with only a thin flexible cable communicating to the outside. Most transducers do not conform very closely to such criteria. Some ceramic hydrophone elements have been produced recently in the form of a sphere about one-inch or less in diameter. One of these might be adapted to a spherical shell of say 25-inch radius to produce an experimental shell model conforming closely to the analytical model. In the case of microphones, commercially-available research systems are quite far removed from the ideal configuration. Possibly an ordinary condenser microphone button might be operated with a field-effect transistor as preamplifier to yield a better packaging. The alternative both in air and in water would be to use a shell sufficiently large so that whatever the transducer's bulk, it was still very small with respect to the shell.

The problem of inserting a transducer into a spherical shell so that the essential aspects of the analytical model are preserved suggests an alternative approach to sonar archetype studies; the more so considering the large physical bulk of sonar transducers compared to the internal volume of a sonar dome. A more realistic model for analysis would be the one shown in Fig. 24. A concentric spherical transducer has been placed inside the spherical shell. Since a completely spherical geometry has been maintained, this model should be tractable to analysis in closed mathematical form just as the spherical shell was. (Other geometries will not permit such a complete solution.) The increased

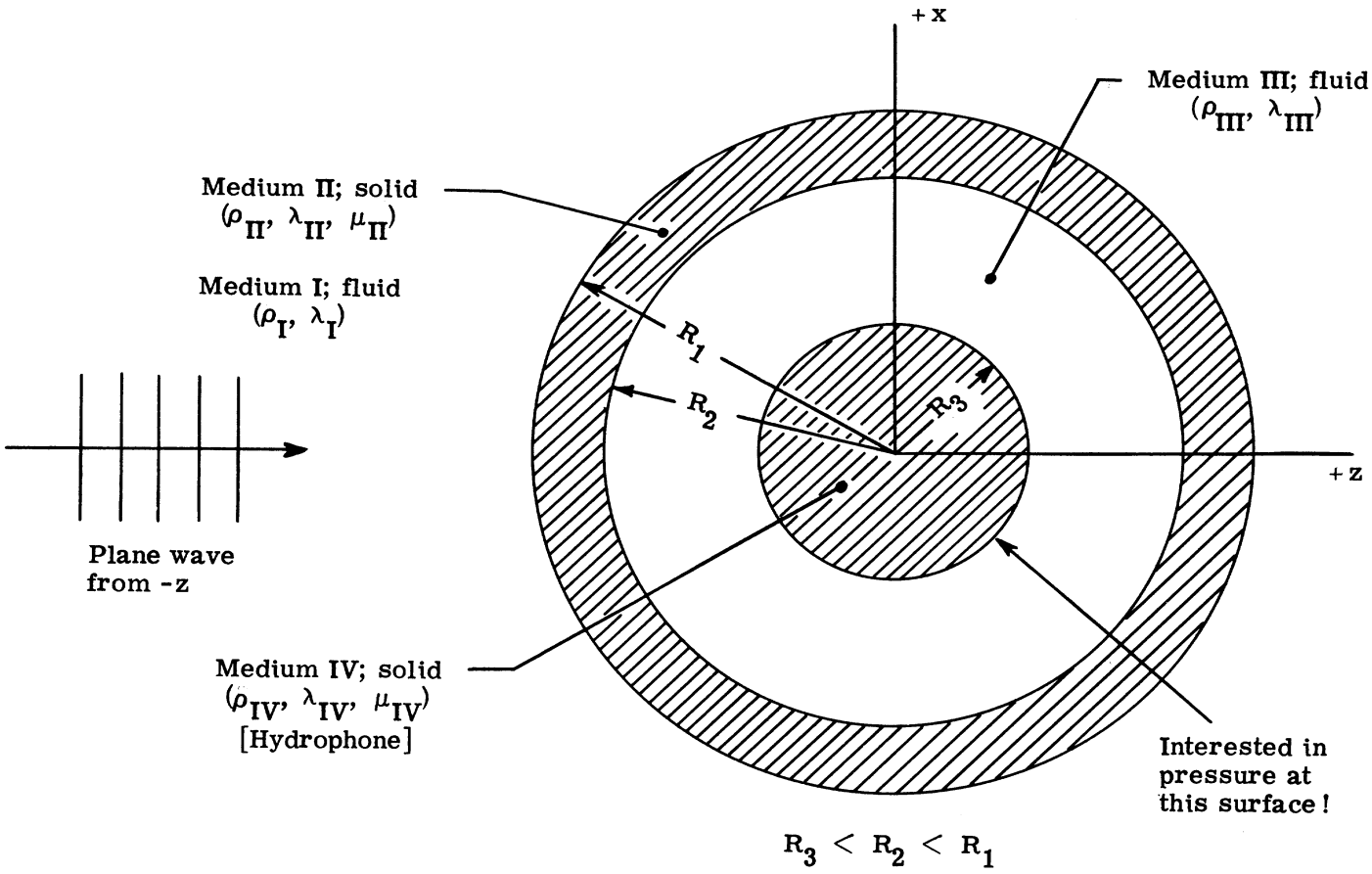

Fig. 24. Proposed new analytical model.

complexity of the new model enters an additional spherical surface on which boundary conditions must be satisfied. This will increase the complexity of the coefficients, but the new complexity is simply algebraic, not fundamental.

In the case of the new model, the spherical transducer would presumably have solid-like material properties. Likewise, one would solve for the acoustical pressure on the surface of the transducer. The transducer's radius could be of arbitrary magnitude as long as it was smaller than the inner radius of the shell. Thus at one stroke, the need for a point acoustical measurement would be relieved and a realistic transducer bulk introduced. It would have been foolhardy to attempt the analysis of such a complicated model initially, but the analytical success achieved with the spherical shell model is reassuring.

In summary, the recommendations for future research are to exploit the computer solution for the spherical-shell problem with appropriate comfirmatory experiments in air, water, and mixed fluids. Then a more complicated model of a spherical transducer surrounded by an immersed spherical shell ought to be analyzed. These investigations are to be accomplished under steady-state conditions. As a final step, it would be desirable to look at pulse shapes for the internal field in a manner similar to Hickling's work (Ref. 7) on the scattered field. Since the shell and the enclosed cavity encompass dynamic behavior characteristics, pulse shapes received inside a shell probably are altered under some circumstances.

APPENDIX A

TERMS IN THE COEFFICIENTS

Using the abbreviations $x = kR$, $x_L = k_L R$, $x_T = k_T R$, $y = k(R - \Delta)$, $y_L = k_L(R - \Delta)$, and $y_T = k_T(R - \Delta)$, the elements of the determinants are given by:

$$a_1 = j_\ell(x)\rho_I / \rho_{II}$$

$$a_2 = x j'_\ell(x)$$

$$\alpha_{11} = h_\ell^{(1)}(x)\rho_I / \rho_{II}$$

$$\alpha_{21} = x h_\ell^{(1)'}(x)$$

$$\alpha_{12} = [\lambda_{II} j_\ell(x_L) - 2\mu_{II} j''_\ell(x_L)] \; / \; (\lambda_{II} + 2\mu_{II})$$

$$\alpha_{22} = x_L j'_\ell(x_L)$$

$$\alpha_{32} = 2[x_L j'_\ell(x_L) - j_\ell(x_L)]$$

$$\alpha_{42} = [\lambda_{II} j_\ell(y_L) - 2\mu_{II} j''_\ell(y_L)] \; / \; (\lambda_{II} + 2\mu_{II})$$

$$\alpha_{52} = y_L j'(y_L)$$

$$\alpha_{62} = 2[y_L j'_\ell(y_L) - j_\ell(y_L)]$$

$$\alpha_{13} = -2\ell(\ell+1)\, x_T^{-2} [x_T j'_\ell(x_T) - j_\ell(x_T)]$$

$$\alpha_{23} = \ell(\ell+1)\, j_\ell(x_T)$$

$$\alpha_{33} = x_T^2 j''_\ell(x_T) + (\ell+2)(\ell-1)\, j_\ell(x_T)$$

$$\alpha_{43} = -2\ell(\ell+1)\, y_T^{-2} [y_T j'_\ell(y_T) - j_\ell(y_T)]$$

$$\alpha_{53} = \ell(\ell+1)\, j_\ell(y_T)$$

$$\alpha_{63} = y_T^{\,2}\, j_\ell''(y_T) + (\ell+2)(\ell-1)\, j_\ell(y_T)$$

$$\alpha_{14} = [\lambda_{II} n_\ell(x_L) - 2\mu_{II} n_\ell''(x_L)] \;/\; (\lambda_{II}+2\mu_{II})$$

$$\alpha_{24} = x_L n_\ell'(x_L)$$

$$\alpha_{34} = 2[x_L n_\ell'(x_L) - n_\ell(x_L)]$$

$$\alpha_{44} = [\lambda_{II} n_I(y_L) - 2\mu_{II} n_\ell''(y_L)] \;/\; (\lambda_{II} + 2\mu_{II})$$

$$\alpha_{54} = y_L n_\ell'(y_L)$$

$$\alpha_{64} = 2[y_L n_\ell'(y_L) - n_\ell(y_L)]$$

$$\alpha_{15} = -2\ell(\ell+1) x_T^{-2} [x_T n_\ell'(x_T) - n_\ell(x_T)]$$

$$\alpha_{25} = \ell(\ell+1)\, n_\ell(x_T)$$

$$\alpha_{35} = x_T^{\,2} n_\ell''(x_T) + (\ell+2)(\ell-1)\, n_\ell(x_T)$$

$$\alpha_{45} = -2\ell(\ell+1)\, y_T^{-2} [y_T n_\ell'(y_T) - n_\ell(y_T)]$$

$$\alpha_{55} = \ell(\ell+1)\, n_\ell(y_T)$$

$$\alpha_{65} = y_T^{\,2} n_\ell''(y_T) + (\ell+2)(\ell-1)\, n_\ell(y_T)$$

$$\alpha_{46} = j_\ell(y)\rho_I \;/\; \rho_{II}$$

$$\alpha_{56} = y j_\ell'(y)$$

APPENDIX B

CORRELATION WITH HICKLING'S COEFFICIENT

Hickling (Ref. 7), in his work with the scattered field from a spherical shell, used an analysis which was similar to that of Goodman and Stern (Ref. 3). However, the elements in Hickling's determinants were arranged and numbered differently as best suited his purposes. Hickling defined a coefficient, F_n, which fulfilled a role rather similar to A^I used by Goodman and Stern. In Ref. 7, Hickling presented tables of some typical numerical values of his F_n. In order to compare out computer program's output with Hickling's for the external scattered field, the following identification was found to hold. It is expressed in the nomenclature of Goodman and Stern and of this report:

$$A_0^I = \frac{a_1 F_0 - a_2}{\alpha_{11} F_0 - \alpha_{21}}$$

$$= \frac{j_0(kR)\frac{\rho_I}{\rho_{II}} F_0 - kRj_0'(kR)}{h_0(kR)\frac{\rho_I}{\rho_{II}} F_0 - kRh_0'(kR)}$$

Thus by running our program for a set of shell dimensions and material parameters used by Hickling and requiring our program to print out A_0^I along with the corresponding values of $j_0(kR)$, $j_0'(kR)$, $n_0(kR)$, and $n_0'(kR)$ which were produced to evaluate the α_{ij}, we could form a comparison value of A_0^I from Hickling's numerical value of F_0. These two values of A_0^I agreed within about two percent.

APPENDIX C

MATERIAL PARAMETERS

Material	Lamé Constants		Density
	λ	μ	ρ
	N/m^2	N/m^2	kg/m^3
Air	0.154E 06	0	0.129E 01
Sea water	0.230E 10	0	0.102E 04
Steel	0.113E 12	0.757E 11	0.770E 04
Aluminum	0.610E 11	0.250E 11	0.270E 04
Brass	0.113E 12	0.380E 11	0.853E 04
Copper	0.131E 12	0.460E 11	0.889E 04
Lucite	0.562E 10	0.143E 10	0.118E 04
Polyester-glass	0.214E 11	0.140E 09	0.180E 04
Pyrex glass	0.230E 11	0.250E 11	0.232E 04

Values obtained principally from Ref. 13.

REFERENCES

1. J. W. Strutt (Lord Rayleigh), The Theory of Sound, vol. 2, p. 272, Dover Publications, New York, 1945. (A reissue of the original 1894 second edition.)

2. V. C. Anderson, "Sound Scattering from a Fluid Sphere," J. Acoust. Soc. Am., vol. 22, p. 426 (1950).

3. R. R. Goodman and R. Stern, "Reflection and Transmission of Sound by Elastic Spherical Shells," J. Acoust. Soc. Am., vol. 34, p. 338 (1962).

4. R. R. Goodman, W. C. Meecham, F. Sevcik, and R. Stern, "The Reflection and Transmission of Sound by Elastic Shells," The University of Michigan, Institute of Science and Technology Report 2784-5-T, December 1960, Ann Arbor, Michigan.

5. Raya Stern, "The Transmission of Sound by a Hemispherical Shell Mounted on a Rigid Plate," The University of Michigan, Institute of Science and Technology Report 2784-6-T, December 1960, Ann Arbor, Michigan.

6. R. Hickling, "Analysis of Echoes from a Solid Elastic Sphere in Water," J. Acoust. Soc. Am., vol. 34, p. 1582 (1962).

7. R. Hickling, "Analysis of Echoes from a Hollow Metallic Sphere in Water, "J. Acoust. Soc. Am., vol. 36, p. 1124, (1964).

8. L. D. Hampton and C. M. McKinney, "Experimental Study of the Scattering of Acoustical Energy from Solid Metal Spheres in Water," J. Acoust. Soc. Am., vol. 33, p. 664 (1961).

9. K. J. Diercks and R. Hickling, "Study of Acoustic Scattering by Hollow Metallic Spheres," J. Acoust. Soc. Am., vol. 37, p. 1176(A), (1965).

10. L. E. Kinsler and A. R. Frey, Fundamentals of Acoustics, Second Edition, John Wiley and Sons, Inc., New York, 1962.

11. C. L. Wakamo, "Low-Frequency Anechoic Tank for Underwater-Sound Studies," The University of Michigan, Institute of Science and Technology Report 2784-8-T, November 1962, Ann Arbor, Michigan.

12. M. Abramowitz and I. A. Stegun, editors, Handbook of Mathematical Functions, National Bureau of Standards Applied Mathematics Series 55, U. S. Government Printing Office, Washington, D. C., June 1964. See Chapter 10.

13. American Institute of Physics Handbook, McGraw-Hill, New York, 1957, Section 3.

DISTRIBUTION LIST

No. of Copies	
2	Office of Naval Research (Code 468) Navy Department Washington, D. C. 20360
6	Director, Naval Research Laboratory Technical Information Division Washington, D. C. 20360
1	Director Office of Naval Research Branch Office 1030 East Green Street Pasadena, California 91101
1	Office of Naval Research San Francisco Area Office 1076 Mission Street San Francisco, California 94103
1	Director Office of Naval Research Branch Office 495 Summer Street Boston, Massachusetts 02210
1	Office of Naval Research New York Area Office 207 West 24th Street New York, New York 10011
1	Director Office of Naval Research Branch Office 219 South Dearborn Street Chicago, Illinois 60604
8	Commanding Officer Office of Naval Research Branch Office Box 39 FPO New York 09510
1	Commander, Naval Ordnance Laboratory Acoustics Division White Oak, Silver Spring, Maryland 20910
1	Director, Ordnance Research Laboratory Pennsylvania State University University Park, Pennsylvania 16801
1	Brown University Research Analysis Group Providence, Rhode Island 02906
1	U. S. Navy SOFAR Station APO, New York 09856 Attn: Dr. G. R. Hamilton
1	Defense Research Laboratory University of Texas Austin, Texas 78712
1	University of Miami Institute of Marine Science #1 Rickenbacker Causeway Miami, Florida 33149
1	Director, Applied Physics Laboratory University of Washington Seattle, Washington 98105
1	Director Marine Physical Laboratory of the Scripps Institution of Oceanography University of California San Diego, California 92152
1	Commanding Officer and Director Navy Electronics Laboratory San Diego, California 92152
1	Chief Scientist Navy Underwater Sound Reference Division Post Office Box 8337 Orlando, Florida 32800
1	Commanding Officer and Director Navy Underwater Sound Laboratory Fort Trumbull New London, Connecticut 06321

DISTRIBUTION LIST (Cont.)

No. of Copies	
1	Hudson Laboratories Columbia University 145 Palisade Street Dobbs Ferry, New York 10522
1	Woods Hole Oceanographic Institution Woods Hole, Massachusetts 02906
1	Institute for Defense Analyses Communications Research Division von Neumann Hall Princeton, New Jersey 08540
1	Commanding Officer Navy Mine Defense Laboratory Panama City, Florida 32402
1	Superintendent Naval Academy Annapolis, Maryland 21402
1	Commander Naval Ordnance Systems Command Code ORD-0302 Navy Department Washington, D. C. 20360
1	Commander Naval Ship Systems Command Code SHIPS-0343 Navy Department Washington, D. C. 20360
1	Commander Naval Ship Systems Command Code SHIPS-1630 Navy Department Washington, D. C. 20360

No. of Copies	
1	Commanding Officer Naval Air Development Center Johnsville, Warminster, Pennsylvania 18974
1	Commanding Officer and Director David Taylor Model Basin Washington, D. C. 20007
1	Superintendent Naval Postgraduate School Monterey, California 93940 Attn: Prof. L. E. Kinsler
1	Commander Naval Ordnance Test Station Pasadena Annex 3203 E. Foothill Boulevard Pasadena, California 91107
1	Dr. H. W. Marsh Manager, Marine Research Department Raytheon Company P. O. Box 128 (33 Union Street) New London, Connecticut 06321
20	Defense Documentation Center Cameron Station Alexandria, Virginia 22314
10	Cooley Electronics Laboratory The University of Michigan Ann Arbor, Michigan 48105

UNCLASSIFIED

Security Classification

DOCUMENT CONTROL DATA - R&D

(Security classification of title, body of abstract and indexing annotation must be entered when the overall report is classified)

1. ORIGINATING ACTIVITY (Corporate author)	2a. REPORT SECURITY CLASSIFICATION
Cooley Electronics Laboratory The University of Michigan Ann Arbor, Michigan	UNCLASSIFIED
	2b. GROUP

3. REPORT TITLE

Attenuation of Sound by Spherical Shells.

4. DESCRIPTIVE NOTES (Type of report and inclusive dates)

Final Report - 2784-9-F

5. AUTHOR(S) (Last name, first name, initial)

Barnett, Norman E.

6. REPORT DATE	7a. TOTAL NO. OF PAGES	7b. NO. OF REFS
October, 1966	79	13

8a. CONTRACT OR GRANT NO.	9a. ORIGINATOR'S REPORT NUMBER(S)
NONR-1224(24) b. PROJECT NO. 185-103 c. d.	2784-9-F 9b. OTHER REPORT NO(S) (Any other numbers that may be assigned this report)

10. AVAILABILITY/LIMITATION NOTICES

"Distribution of this Document is Unlimited"

11. SUPPLEMENTARY NOTES	12. SPONSORING MILITARY ACTIVITY
	Department of the Navy Office of Naval Research Washington, 25, D. C.

13. ABSTRACT

The study of acoustic attenuation at low frequencies by thin spherical shells was continued beyond the initial analysis by Goodman and Stern (J. Acoust. Soc. Am., 34:338, 1962). Experimental measurements were conducted both in air and in water. Numerical evaluation was extended to include the first-order coefficient. For metallic shells immersed in either air or water, the first-order coefficient is larger than, and exhibits interesting fluctuations at lower frequencies than, the zeroth-order coefficient. As a practical consequence, pure zeroth-order behavior is difficult to observe even in the laboratory and most measurements exhibit the combined effects from several orders.

DD FORM 1 JAN 64 1473

UNCLASSIFIED

Security Classification

14. KEY WORDS	LINK A		LINK B		LINK C	
	ROLE	WT	ROLE	WT	ROLE	WT

INSTRUCTIONS

1. ORIGINATING ACTIVITY: Enter the name and address of the contractor, subcontractor, grantee, Department of Defense activity or other organization *(corporate author)* issuing the report.

2*a*. REPORT SECURITY CLASSIFICATION: Enter the overall security classification of the report. Indicate whether "Restricted Data" is included. Marking is to be in accordance with appropriate security regulations.

2*b*. GROUP: Automatic downgrading is specified in DoD Directive 5200.10 and Armed Forces Industrial Manual. Enter the group number. Also, when applicable, show that optional markings have been used for Group 3 and Group 4 as authorized.

3. REPORT TITLE: Enter the complete report title in all capital letters. Titles in all cases should be unclassified. If a meaningful title cannot be selected without classification, show title classification in all capitals in parenthesis immediately following the title.

4. DESCRIPTIVE NOTES: If appropriate, enter the type of report, e.g., interim, progress, summary, annual, or final. Give the inclusive dates when a specific reporting period is covered.

5. AUTHOR(S): Enter the name(s) of author(s) as shown on or in the report. Enter last name, first name, middle initial. If military, show rank and branch of service. The name of the principal author is an absolute minimum requirement.

6. REPORT DATE: Enter the date of the report as day, month, year; or month, year. If more than one date appears on the report, use date of publication.

7*a*. TOTAL NUMBER OF PAGES: The total page count should follow normal pagination procedures, i.e., enter the number of pages containing information.

7*b*. NUMBER OF REFERENCES: Enter the total number of references cited in the report.

8*a*. CONTRACT OR GRANT NUMBER: If appropriate, enter the applicable number of the contract or grant under which the report was written.

8*b*, 8*c*, & 8*d*. PROJECT NUMBER: Enter the appropriate military department identification, such as project number, subproject number, system numbers, task number, etc.

9*a*. ORIGINATOR'S REPORT NUMBER(S): Enter the official report number by which the document will be identified and controlled by the originating activity. This number must be unique to this report.

9*b*. OTHER REPORT NUMBER(S): If the report has been assigned any other report numbers *(either by the originator or by the sponsor)*, also enter this number(s).

10. AVAILABILITY/LIMITATION NOTICES: Enter any limitations on further dissemination of the report, other than those imposed by security classification, using standard statements such as:

(1) "Qualified requesters may obtain copies of this report from DDC."

(2) "Foreign announcement and dissemination of this report by DDC is not authorized."

(3) "U. S. Government agencies may obtain copies of this report directly from DDC. Other qualified DDC users shall request through _____."

(4) "U. S. military agencies may obtain copies of this report directly from DDC. Other qualified users shall request through _____."

(5) "All distribution of this report is controlled. Qualified DDC users shall request through _____."

If the report has been furnished to the Office of Technical Services, Department of Commerce, for sale to the public, indicate this fact and enter the price, if known.

11. SUPPLEMENTARY NOTES: Use for additional explanatory notes.

12. SPONSORING MILITARY ACTIVITY: Enter the name of the departmental project office or laboratory sponsoring *(paying for)* the research and development. Include address.

13. ABSTRACT: Enter an abstract giving a brief and factual summary of the document indicative of the report, even though it may also appear elsewhere in the body of the technical report. If additional space is required, a continuation sheet shall be attached.

It is highly desirable that the abstract of classified reports be unclassified. Each paragraph of the abstract shall end with an indication of the military security classification of the information in the paragraph, represented as *(TS), (S), (C), or (U)*.

There is no limitation on the length of the abstract. However, the suggested length is from 150 to 225 words.

14. KEY WORDS: Key words are technically meaningful terms or short phrases that characterize a report and may be used as index entries for cataloging the report. Key words must be selected so that no security classification is required. Identifiers, such as equipment model designation, trade name, military project code name, geographic location, may be used as key words but will be followed by an indication of technical context. The assignment of links, rules, and weights is optional.